ELSEVIER

Marine and Petroleum Geology 20 (2003) 649–676

Marine and Petroleum Geology

www.elsevier.com/locate/marpetgeo

Architecture and evolution of upper fan channel-belts on the Niger Delta slope and in the Arabian Sea

Mark E. Deptuck[a,*], Gary S. Steffens[b], Mark Barton[b], Carlos Pirmez[b]

[a]*Department of Earth Sciences, Dalhousie University, Halifax, Nova Scotia, Canada B3J 4J1*
[b]*Turbidite Research Team, Shell International Exploration and Production, Inc., 3737 Bellaire Blvd., Houston, TX 77025, USA*

Received 1 July 2002; accepted 8 January 2003

Abstract

High-resolution multichannel 2-D and 3-D seismic data, primarily from upper fan reaches of near-seafloor channel-levee systems on the Niger Delta slope and in the Arabian Sea, reveal a high level of detail and architectural complexity. Several architectural elements are common to each system examined in this study. They include inner levees, outer levees, erosional fairways, channel-axis deposits, rotational slumps blocks, and mass transport deposits. Although the scale of individual systems varies significantly, similarities in first-order architectural elements and their configurations suggest that common depositional processes are involved regardless of scale differences.

Most of the channel-levee systems examined in this study are characterized by a basal erosional fairway that is bordered by outer levees of varying thickness. Together these elements define the base and margins of the channel-belt, where channel-axis deposits and inner levees are the dominant architectural elements. Vertical, sub-vertical, and lateral stacking patterns of sinuous and/or meandering channels create seismic facies that range from narrow to wide zones of high amplitude reflections (HARs) with chaotic to continuous and shingled to horizontal reflections. Some HARs appear as isolated or stacked asymmetric to symmetric u- and v-shaped reflections, referred to here as channel-forms. Channel-belts evolve within the confines of the scalloped erosional fairway walls (flanked by outer levee), and are similar in morphology to meander-belts in fluvial systems, but commonly have a greater component of vertical aggradation. Detailed study of one particular channel-levee system on the Niger Delta slope shows a period of incision followed by three distinct phases of channel development during its aggradational history. Each fill phase corresponds to a different channel stacking architecture, planform geometry, and nature of terrace development, with important implications for reservoir architecture. In some cases, multiple phases of inner levee growth are observed, each intimately linked to the channel migration and aggradation history. Channel sinuosity evolves dynamically, with some meander loops undergoing periods of accelerated meander growth at the same time that others show little lateral migration.

Keywords: Channel-levee systems; Channel-belt; Upper fan; Architecture; Sinuous channel; Inner levee; Planform evolution

1. Introduction

Submarine channels flanked by levees have been recognized as important components of deep water systems since the early work done by Normark (1970, 1978) and Walker (1978) and many others. Channel-levee systems dominate the upper fan architecture of most large- and medium-sized submarine fans, including the Mississippi (Bouma, Coleman, & DSDP Leg 96 Shipboard Scientists, 1985), Amazon (Damuth & Flood, 1985), Indus (McHargue & Webb, 1986; Kolla & Coumes, 1987), Bengal (Emmel & Curray, 1985), Zaire (Droz, Rigaut, Cochonat, & Tofani, 1996), Toyama (Nakajima, Satoh, & Okamura, 1998), and Rhone (Bellaiche et al., 1984), and also many smaller fans like Hueneme (Piper, Hiscott, & Normark, 1999) and Golo (Bellaiche, Droz, Gaullier, & Pautot, 1994). They act as conduits through which clastic sediment is transported into the deep sea, and they provide confining and sorting mechanisms that allow sand to reach the basin plain. Channel-levee systems also form important repositories for coarse-grained sediment deposited along channel-axes (Bouma et al., 1985; Manley, Pirmez, Busch, & Cramp, 1997) and for fine-grained sands and silts deposited on levees (Hiscott, Hall, & Pirmez 1997; Piper & Deptuck, 1997). For these reasons, the architecture and evolution of channel-levee systems are of interest to the petroleum industry.

* Corresponding author. Tel.: +1-902-426-6737.
E-mail address: mdeptuck@dal.ca (M.E. Deptuck).

0264-8172/$ - see front matter © 2003 Elsevier Ltd. All rights reserved.
doi:10.1016/j.marpetgeo.2003.01.004

Studies on channel-levee architecture in the shallow and deep subsurface are sometimes hindered by problems related to poor data-quality (e.g. problems imaging channel-axis deposits due to sideswipe (Flood, 1987) and diffraction from channel walls in single channel or poorly migrated data) or insufficient channel-levee thickness to reveal detailed internal architecture. These issues hamper the study of channel evolution and in particular make it difficult to assess how submarine channels migrate through time and the importance of point bars and inner levees. Resolving these issues is important for developing improved reservoir models that better predict baffles and barriers to fluid flow.

This study focuses on two locations—the Arabian Sea and the Niger Delta slope—where high-quality industry seismic data cover the proximal reaches of several large channel-levee systems (i.e. immediately outboard the canyon mouth). A vertical seismic resolution of 6–7 m, combined with the large size of the channel-levee systems, provide a unique opportunity to study their evolution and architecture. A detailed 3-D seismic morphological study of one channel-levee system on the Niger Delta slope provides details about the evolution of channel-axis deposits and inner levees that have not previously been recognized.

We define a channel-levee system (abbreviated to CLS) as a single channel-belt, bordered by outer levees. We define a channel-levee complex (abbreviated to CLC) as a series of stacked channel-levee systems that are fed by the same canyon. Incision of a new canyon, therefore, results in the deposition of a new CLC, and is a first order control on fan architecture. A similar convention was used in studies of the Amazon Fan (e.g. Damuth & Flood, 1985). The term high amplitude reflections (HARs) is used in this study to describe high amplitude seismic reflections located within the channel-belt. HARs are believed to correspond to coarser-grained lithologies associated with the fill of aggrading or laterally migrating channel-axes (e.g. Damuth, Kowsmann, Flood, Belderson, & Gorini, 1983; Kastens & Shor, 1985). Core calibration from the Mississippi and Amazon fans confirms the coarser-grained nature of HARs (Bouma et al., 1985; Manley et al., 1997). As will be discussed, some HARs within the channel-belt correspond to deposits above terraces that are not directly related to channel-axis deposits. The term channel-axis deposit is used in this study to describe deposits on the floor of the channel, near its axis but not exclusively along the thalweg. Channel-axis deposits are commonly wider than the true axis or thalweg of the system, but show a similar planform geometry.

2. Indus Fan—Arabian Sea

The Indus Fan is a large, river-fed submarine fan (Kenyon, Amir, & Cramp, 1995), second in size only to the Bengal Fan on the opposite side of India. It was deposited in a predominantly unconfined setting on the continental slope, rise, and basin floor, covering much of the Arabian Sea. The entire fan extends over an area of 1.1×10^5 km^2 with greater than 9 km of sediment accumulating near the toe-of-slope (Kolla & Coumes, 1987; Clift et al., 2001). Fan sedimentation is estimated to have begun at the end of the Oligocene or beginning of the Miocene, during Himalayan uplift (Kolla & Coumes, 1987; McHargue & Webb, 1986; Clift et al., 2001).

The upper Indus Fan, both past and present, consists of some of the largest CLSs observed. They have been studied by several authors using a variety of data types, ranging from multichannel industry seismic data to 3.5 kHz single channel seismic data and shallow piston cores (e.g. Naini & Kolla, 1982; McHargue & Webb, 1986; Kolla & Coumes, 1987; Droz & Bellaiche, 1991; McHargue, 1991). Three canyon incisions have been reported on the shelf and slope, including the modern Indus Canyon and two ancestral canyons located further west. Outboard of these canyons, much of the upper 3 km of strata consists of stacked CLCs, each consisting of two or more CLSs.

2.1. Seismic data set

Just west of the modern Indus Canyon, 2042 line kilometers of excellent quality 2-D seismic data from two different vintages (1999 and 1977-reprocessed in 1999) were used. The data set covers an area similar to that studied by McHargue and Webb (1986), but with a tighter grid spacing (Fig. 1). The 1999 data set is 120-fold, with frequency roll-off at near 80 Hz (approximately a 6 m vertical resolution). The reprocessed 1977 data set, combined with the 1999 data set, yield a grid spacing ranging from 2.5 to about 8 km. Coverage extends from the shelf in less than 100 m of water to near the base-of-slope at present-day water depths of 1700 m (Fig. 1). These data provide detailed information about the distribution and architecture of CLSs to subsurface depths of more than 3 km.

2.2. Channel-levee complex C

CLC C is the largest in our study area and has the best seismic coverage (Fig. 1). It is draped by 250–300 m of strata consisting of continuous and parallel seismic facies. CLC C consists of three CLSs (C1, C2, and C3—Fig. 1) that stack both laterally and vertically to produce a maximum composite thickness of 950 ms (twt). Assuming an interval velocity of 2100 m/s (extrapolated from Kolla & Coumes, 1987), this would yield a maximum thickness of about 1000 m. The stacking pattern of C1, C2, and C3 produces an overall fan-shaped planform geometry extending from the mouth of ancestral canyon C. The width of the complex increases from about 30 km near the canyon mouth to greater than 80 km near the distal limits of the study area (where the CLSs are laterally offset from one

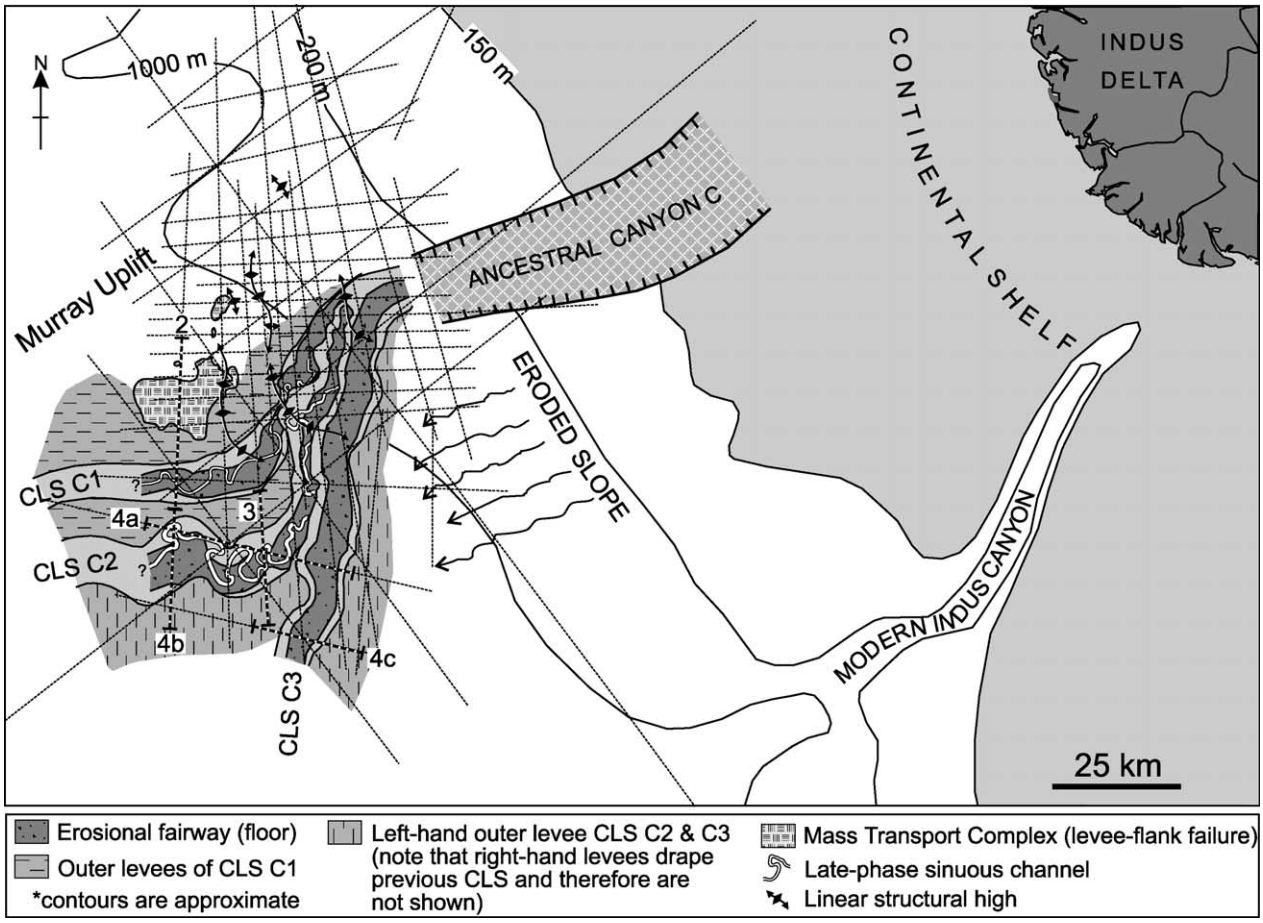

Fig. 1. Indus upper fan with location of 2-D seismic data, channel-levee systems (CLSs) C1, C2, and C3, and figure locations. Also shown is the planform geometry of two distinctive narrow HARs discussed in text.

another—Fig. 1). CLS C1 was deposited furthest west, and each successive system (C2 and C3) was deposited further east.

CLC C has been studied previously by McHargue and Webb (1986—their canyon-channel system C, Ca, Cb) and Kolla and Coumes (1987—their canyon 2 and channels 2a, 2b, 2c) using a sparser grid of data. Their results were particularly useful for confirming the location of the feeder canyon (ancestral canyon C) most of which lies just outside our study area. Tighter line spacing and improved data quality allows us to build on their work and to draw important comparisons with CLSs in other settings (e.g. Niger Delta slope).

Precise age control for CLC C is not available. Onlap relationships, however, indicate that the complex postdates the Early Miocene uplift of the Murray Ridge (Fig. 1), a structural high located along the northern margin of the study area (see also Clift et al., 2001 and references therein). Both Kolla and Coumes (1987) and Clift et al. (2001) used well data from the shelf for additional age control. Kolla and Coumes (1987) inferred that the complex (their canyon 2) was active in the Pliocene, whereas jump ties to seismic profiles from Clift et al. (2001) suggest the complex was active in the Late Miocene, therefore providing only a rough estimate of its age (Late Miocene and/or Pliocene).

2.3. Architecture of individual channel-levee systems

CLSs C1, C2, and C3 each have a maximum thickness of about 750 ms (twt), a width of about 30 km and a distance of roughly 8–10 km between the outer levee crests. Several common architectural elements are recognized in each system. The elements most pertinent to the channel-belt and most easily recognized on 2-D seismic data include the erosional fairway (defines the base of the channel-belt), outer levees (provide additional lateral confinement for the channel-belt), inner levees, and channel-axis deposits (expressed as HARs).

2.3.1. Erosional fairway element

The erosional fairway element is a canyon-like incision flanked by wedge-shaped outer levees, typically found on the middle to lower slope (Figs. 2–4). The up-dip limit of the erosional fairway (i.e. the canyon mouth) is defined as the position along the canyon where outer levees are first

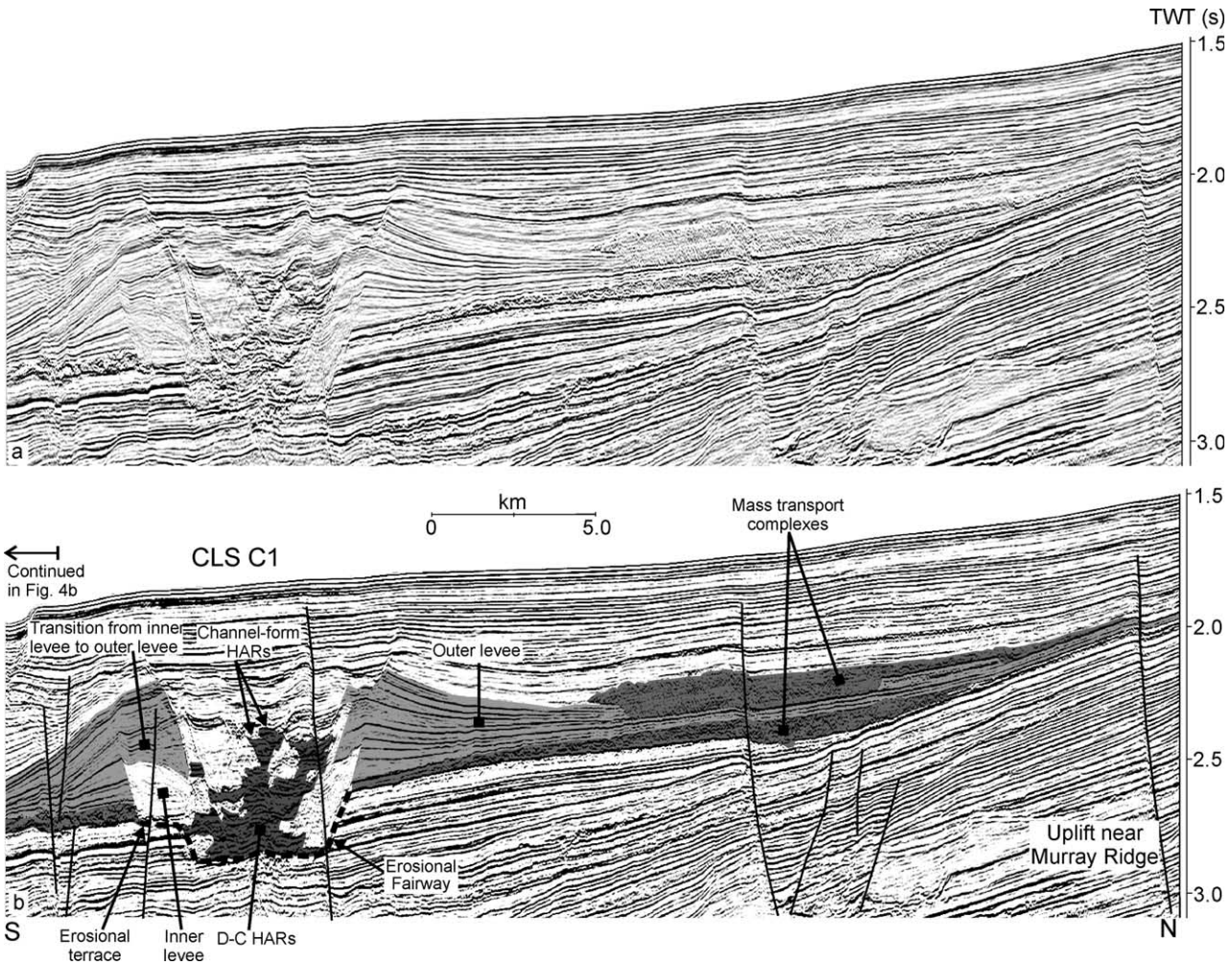

Fig. 2. (a) Uninterpreted and (b) interpreted seismic profile across CLS C1 showing the first-order architectural elements (erosional fairway, inner levees, outer levees, and various types of HARs corresponding to channel deposits). Note the sharp contacts between inner and outer levees. Profile location and the inferred planform geometry of the narrow channel-form (near top of HARs) are shown in Fig. 1.

recognized. Its distal limit is defined where erosion is no longer recognized at the base of the system.

The erosional fairway element in systems C1, C2, and C3 ranges in depth from less than 200 to over 600 m and in width from approximately 5 to 8 km. Generally, the deepest incision is observed nearest the canyon mouth or where the erosional fairway cuts through positive bathymetric features on the sea floor (e.g. where CLS C3 erodes through an older CLS—Fig. 4(c)). In contrast, shallowest incision is observed within structural sags and distally (i.e. furthest away from the canyon mouth).

Deposits within erosional fairways range from high amplitude facies associated with channel-axis deposits, to lower amplitude facies associated with chaotic mass transport deposits, rotational slump blocks, and inner levees.

2.3.2. Outer levee element

The most common and diagnostic elements on the Indus Fan are outer levees (Figs. 2–4), believed to form from the overbanking of predominantly fine-grained sediment during the passage of turbidity currents (Naini & Kolla, 1982). Their original external depositional geometry is wedge-shaped, converging away from the axis of the erosional fairway. They reach a maximum thickness of over 500 m at the crest, and thin to less than 100 m on the flank, over distances of around 10 km.

Seismic reflections within outer levees are almost always continuous, but can range from low to high amplitude. Individual seismic reflections show an increase in dip as outer levees aggrade. Near the southern edge of the study area, where outer levees are best developed, they show an increase in maximum dip from less than 2° (at their base) to greater than 5° (at the top). Seismic reflections within outer levees may also show internally developed downlap and apparent toplap surfaces.

2.3.3. Inner levee element

Von Rad and Tahir (1997) noted the occurrence of muddy bench-like depositional ‘terraces’ within the modern Indus Canyon, at several stepped levels above the channel

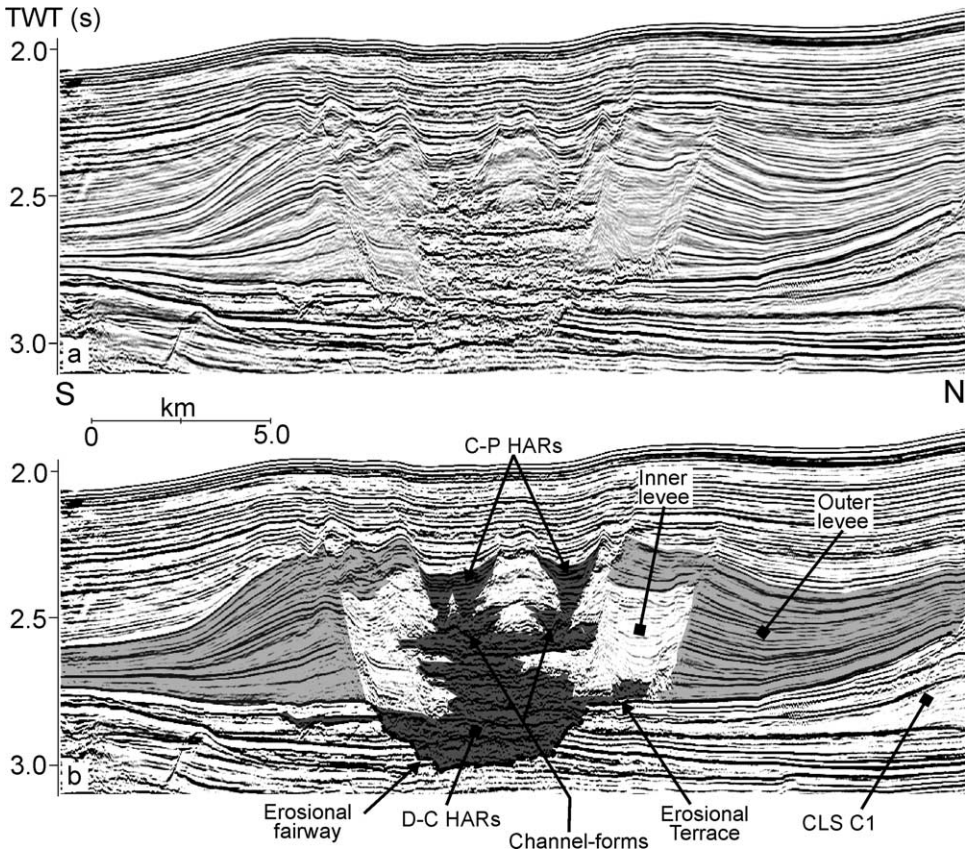

Fig. 3. (a) Uninterpreted and (b) interpreted seismic profile across CLS C2 showing the principal architectural components identified in CLSs in this study. Note the sharp contact between the roughly symmetrical outer levees and the channel-belt (consisting of inner levees and HARs). Note also the prominent erosive base (erosional fairway) and that the HARs are wider near the base of the system and narrower at the top. Fig. 1 shows location and the planform geometry of the narrow C-P HARs at the top of the system. Other profiles crossing the same C-P HARs are shown in Figs. 4(a) and (b).

floor, ranging from 80 to 360 m. Hubscher, Spieb, Breitzke, & Weber (1997) recognized similar features on the Bengal Fan and referred to them as inner levees. Similar 'terrace' forming features are also recognized in many of the buried systems of the Indus Fan, and were referred to by McHargue (1991) as overbank deposits from thalweg channels. We interpret most of these features as inner levees (following the terminology of Hubscher et al., 1997), and interpret them to form from both depositional processes (i.e. vertical aggradation of inner levee deposits resulting from the overbanking of under-fit channels) and erosional processes (i.e. sculpting and slumping of inner levees along channel margins).

Inner levees are common and easily recognized on the upper Indus Fan, where they form quadrilateral shapes likes squares, rectangles or parallelograms in vertically exaggerated seismic cross-sections (e.g. Figs. 2–4). They may also form irregular shapes, particularly on traverses crossing the inside bend of meander loops (e.g. Fig. 4(a)) and wedge-shaped geometries, particularly in areas of reduced confinement. They are typically less than 3 km wide on the Indus Fan, and usually cannot be mapped with confidence for down-channel distances greater than 6 km. Inner levee elements are commonly bordered by sharply defined erosive surfaces that are generally inclined at less than 25 degrees. Erosive interfaces are observed between inner levees and outer levees, between different periods of inner levee growth, and also at boundaries between inner levees and channel-axis deposits, particularly at cut-banks.

2.3.4. Channel and channel-fill elements (HARs)

Channel and channel-fill elements (Mutti and Normark, 1991) are found primarily between the crests of outer levees. Since the channels in CLSs C1, C2, and C3 are no longer active, seismic data record the deposits that accumulated on the channel floor (near its axis) during channel aggradation and migration. McHargue and Webb (1986) described the multi-channel reflection seismic character of 'channel-axis' deposits in CLSs C1, C2, and C3 as high amplitude and discontinuous (H-D). In this study, the H-D seismic facies of McHargue and Webb (1986) are broken down into three distinct HAR seismic facies types: D-C HARs, C-P HARs, and channel-form HARs.

D-C HARs are the most common of the three, consisting of intervals of discontinuous and chaotic seismic reflections, locally containing continuous reflections that look like broad scours (e.g. Figs. 3 and 5(a)). In cross-section, D-C HARs vary in width from less than 1 km to greater than

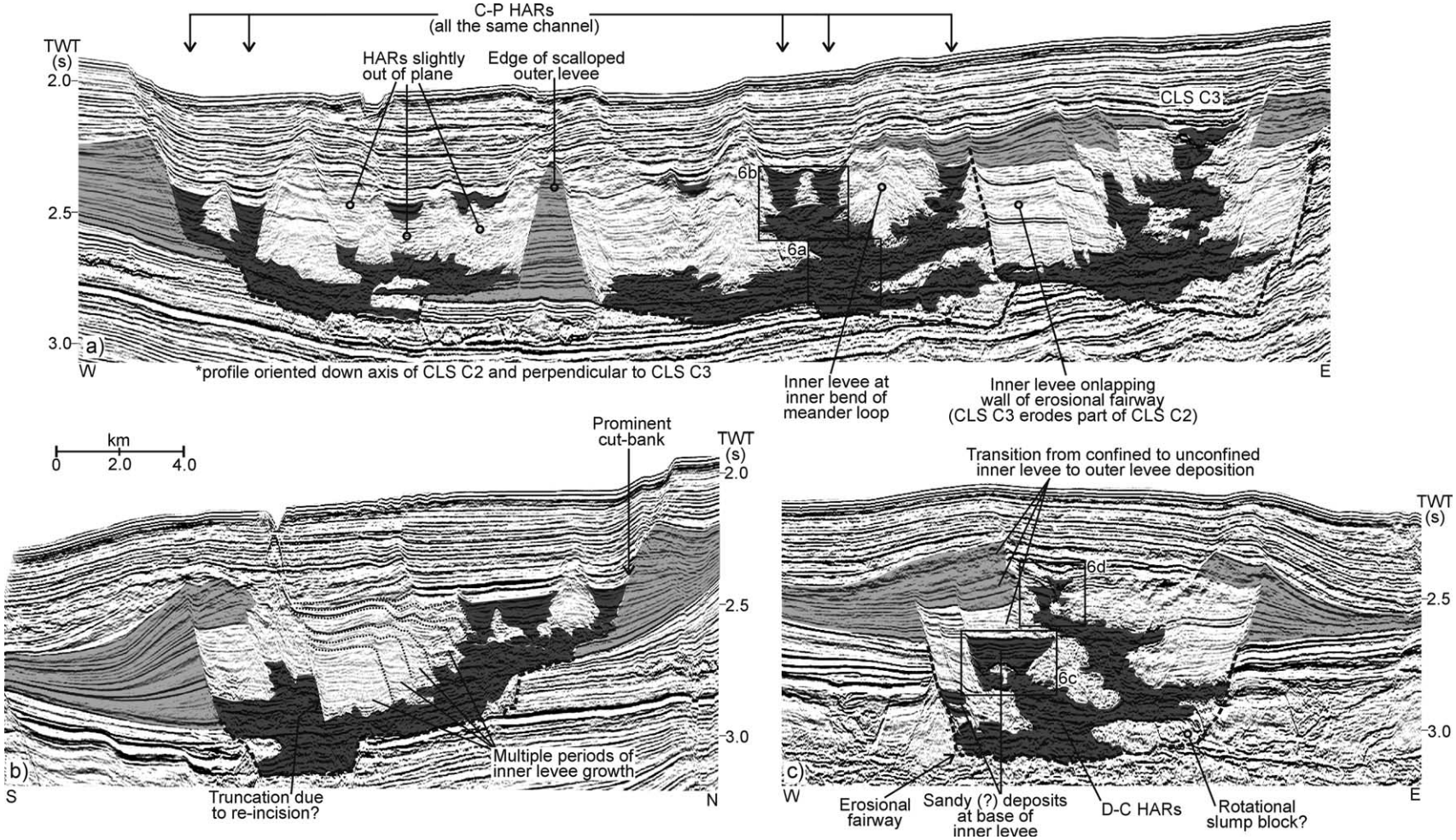

Fig. 4. (a) Interpreted seismic profile traversing perpendicular to CLS C3, and roughly down the axis of CLS C2, showing a complicated 'cactus-like' HARs, and the repetitive crossings of the same sinuous narrow C-P HARs (inferred planform geometry shown in Fig. 1). Note the sharp erosive contact between CLSs C2 and C3. CLS C3 probably experienced several periods of re-incision. (b) Interpreted seismic profile oblique to CLS C2, showing multiple phases of inner levee growth developed opposite a prominent cut-bank. Much of the outer levee has been eroded at the cut-bank. (c) Interpreted seismic profile across CLS C3 showing a rather complex channel-belt architecture. Note the transition from confined inner levees, to unconfined inner levees, and eventually to outer levees as the system aggraded and eventually healed over the prominent incision at the base of the system. Note also the continuous HARs within, and near the base of, the inner levees on both the left and right side of the channel-belt (interpreted as a sandy deposits within the inner levees). See Fig. 1 for locations.

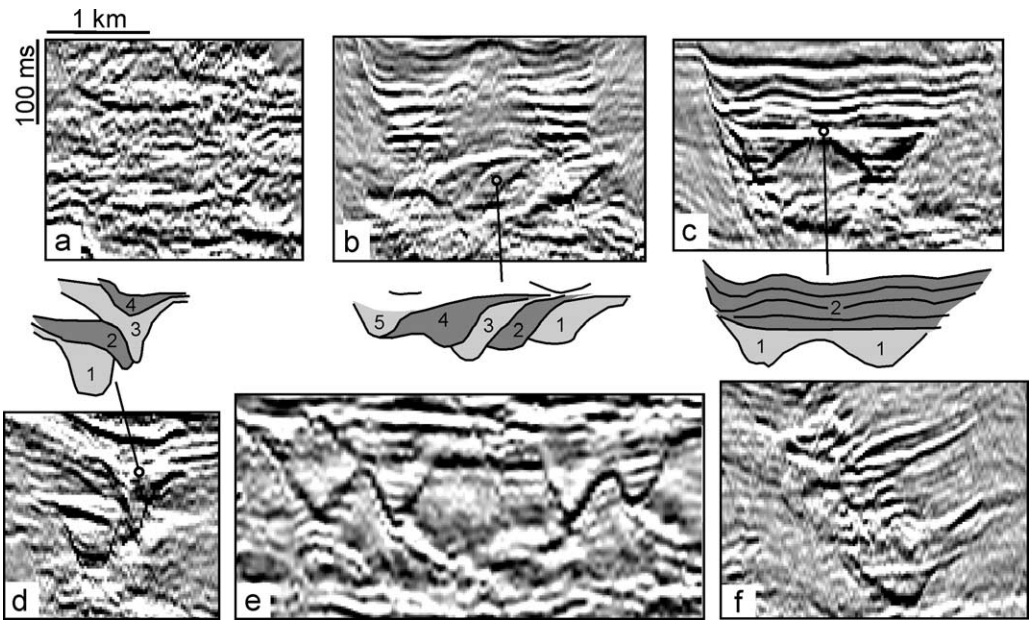

Fig. 5. Seismic profiles illustrating different characteristics of HARs on Indus Fan. (a) Discontinuous to chaotic (D-C) HARs from CLS C2. (b) Profile from CLS C2 showing D-C HARs (at base) passing up-section into laterally migrating cut-and-fill channel-forms (middle), that in turn pass up-section into two limbs of the same narrow continuous and parallel (C-P) HARs (at top). The interval in the middle of the profile consists of at least five separate, partially preserved channel-forms that developed as the channel migrated left through alternating periods of cut-and-fill (line drawing below). Note the inclined events representing second order erosion surfaces that separate each period of cut-and-fill (1–5). No vertical aggradation is observed because the amount of incision between, is approximately equivalent to the amount of deposition within, each channel-form. (c) Profile from CLS C3 showing D-C HARs (base) passing up-section into a channel-form (crossed twice - 1). The channel-form was abandoned and draped by parallel continuous reflections (2), interpreted to be sand-prone deposits within a meander cut-off or above an erosional terrace. These deposits pass up-section into an inner levee (shown in Fig. 4(c)). (d) Four stacked channel-forms separated by second order erosive surfaces. In this case the amount of incision between channel-forms is less than the amount of deposition within each channel-form, resulting in overall aggradation. Location shown in Fig. 4. (e) Profile through CLS C2, crossing the same isolated channel-form four times, indicating that it has a sinuous planform geometry. (f) Profile through a hybrid of narrow aggradational D-C and channel-form HARs from a smaller CLS that underlies CLS C1. The HARs in this example are flanked directly by outer levees, rather than inner levees, because the system lacks an erosive base. See text for details.

5 km, and are commonly wider near the base of the system, within the erosional fairway, than the top. McHargue (1991) interpreted these high amplitude, largely discontinuous seismic facies as coarse-grained thalweg deposits from laterally migrating channels that underwent little vertical aggradation. He reasoned that such deposits could have formed from braided channels. D-C HARs located stratigraphically higher up in the CLSs tend to be narrower and are bordered by prominent inner levees. Such deposits probably originated from the vertical aggradation of sinuous channel (McHargue, 1991). For the most part, the deposits forming D-C HARs do not preserve the original cross-sectional geometry of the channels inferred to have formed them.

In contrast, channel-form HARs (channel-forms, for short) consist of isolated or stacked u- to v-shaped reflections (e.g. Fig. 5(b)–(f)). Each channel-form is defined by a single continuous to discontinuous HAR, inferred to originate from the impedance contrast between deposits below the erosive floor and walls of the channel, and the deposits that partially filled the channel. Channel-forms are therefore interpreted as partially filled second-order incisions, located within the first-order incision of the erosional fairway. Channel-form geometry may be symmetrical or skewed towards the direction of channel migration. Some channel-forms are capped by a single horizontal to sub-horizontal HAR. On some profiles, only partial channel-forms are preserved where they are eroded by an overlying or adjacent one. Channel-forms that stack adjacent to one another may form a series of shingled events inclined in the direction of channel migration. The inclined events are interpreted to correspond to the remnants of channel-forms preserved after several periods of cut-and-fill, the result of abrupt channel migrations (e.g. Fig. 5(b)). Channel-forms that stack vertically may also incise one another (e.g. Fig. 5(d)). Successive channel-forms will aggrade if the amount of incision between channel-forms is less than the thickness of sediment that accumulates within them. Some inclined events may also be generated from point-bar like deposits that result from gradual channel migration (see Abreu, Sullivan, Mohrig, & Pirmez, 2003), although they are not widely recognized in our study area.

In CLC C, channel-form HARs are most common in stratigraphically higher positions within each CLS. For example, an isolated channel-form is observed near the top of CLS C1. Based on repeated crossings on single linear

seismic profiles (as many as four—Fig. 5(e)), it is inferred to have a sinuous planform geometry (shown in Fig. 1). Aside from the tentative recognition of concordant, transparent or chaotic stratal patterns within each channel-form, a more detailed understanding of channel-form fill would require higher resolution seismic and/or core data.

C-P HARs, consisting of intervals of continuous and parallel (to sub-parallel) seismic reflections, are fairly rare within channel-belts in the study area. In CLS C2, vertical profiles cross individual limbs of the distinctive C-P HARs several times (e.g. Figs. 3–5(b)), suggesting a sinuous planform geometry (shown in Fig. 1). Each 'limb' consists of a number of stacked continuous horizons that resemble very shallow relief (flat-lying) channel-forms, interpreted as channel-floor deposits (Fig. 5(b)). No lateral offset is observed between successive reflections, suggesting that little lateral migration occurred during aggradation. The successive widening of reflections, combined with the lack of lateral migration, suggests that the C-P HARs in this example developed during the gradual abandonment of the system, as the remaining channel-relief was filled.

Commonly, the deposits from migrating and aggrading channels produce a hybrid of D-C, C-P, and channel-form HARs. Obviously, distinguishing between the three different HAR facies types requires well processed seismic data, and at higher seismic frequencies (i.e. greater than 80 Hz), more facies types will be recognized (including different stratal fill patterns within individual channel-forms).

Data from the proximal Indus Fan provide useful two-dimensional information about the architecture of large CLSs in upper fan settings, but questions still remain about the three dimensional character of HARs and other elements, as well as their temporal evolution. Detailed 3-D seismic investigations were used to study the cross-sectional and planform architecture and evolution of the Benin-major CLS, located on the western Niger Delta slope. The Benin-major CLS has a similar architecture as the systems described above and therefore provides new insight into observations made from 2-D seismic data.

3. Benin-major CLS

The Niger Delta is located along the western margin of Africa in the Gulf of Guinea. It covers an area of about 75 000 km^2 and consists of a prominent regressive clastic wedge supplied by the modern Niger River and its ancestral counterparts (Doust & Omatsola, 1989). The second study area is located on a relatively undeformed portion of the western Niger Delta slope, between water depths of 850 and 1900 m (Fig. 6). The Benin-major CLS, named here because of its up-dip proximity to the modern Benin River (as identified by Allen, 1964), is located within the upper 500 ms of strata in the study area (Figs. 6–8). The precise age of the system is uncertain, but given its shallow burial depth, it is believed to have been active in the Pleistocene.

3.1. Data and methodology

A large 3-D seismic volume, located on the mid-slope of the western Niger Delta, covers an area of 1250 km^2 (25×50 km^2). Bin spacing is 25×12.5 m^2 and frequency roll-off is near 65 Hz (approximately a 7 m vertical resolution). The 3-D seismic volume captures a 54 km long segment of the Benin-major CLS. The data also encompass a much smaller, slightly older CLS, herein named the Benin-minor CLS. The most detailed study was carried out on a smaller subset of the 3-D seismic survey covering an area of 360 km^2 and a 23 km long segment of the Benin-major CLS, between 850 and 1400 m of water (Fig. 6).

Both amplitude and dissemblance 3-D seismic volumes were used to interpret the Benin-major CLS. Because the slope has a dip of about 1°, the modern sea floor was used as a datum for flattening and to generate horizon-slices. In the detailed study area, the Benin-major CLS has little remaining bathymetric expression and the sea floor marker is relatively flat lying (Figs. 6 and 7(b)). To eliminate local irregularities, a smoothing filter was applied to the horizon. Mapping of individual stacked channel-forms within the detailed study area confirms that their thalwegs are roughly parallel to the modern sea floor. Therefore, when the sea floor horizon is used to generate horizon-slices, it crosses roughly the same stratigraphic position within each stacked channel-form.

3.2. General channel-levee architecture

The Benin-major CLS has a maximum thickness of 450 ms (about 350 m–at the channel-axis), and a distance of 3.0–4.5 km between outer levee crests. It is therefore about half the width and thickness of the CLSs described earlier for the Indus Fan. Similar to the CLSs on the Indus Fan, it consists of an erosional fairway at its base, and is bordered by outer levees. These elements confine the channel-belt comprised of inner levees, channel-axis deposits, coherent rotated slump blocks, and incoherent slump masses (Fig. 8). The erosional fairway is about 170 m deep in the detailed study area, reaching 295 m deep near the western limit of the 3-D seismic volume (west of the detailed study area).

Outer levees have a maximum thickness of about 200 m and consist of continuous moderate to low amplitude seismic reflections that converge away from the channel-axis. They are similar to, but less steep than, the outer levees on the Indus Fan. A prominent, high amplitude seismic marker, mapped across both the eastern and western outer levees, separates it into a lower unit and an upper unit (Fig. 8(a)). The lower outer levee consists of dominantly continuous seismic events. The upper outer levee contains some discontinuous seismic events and has locally

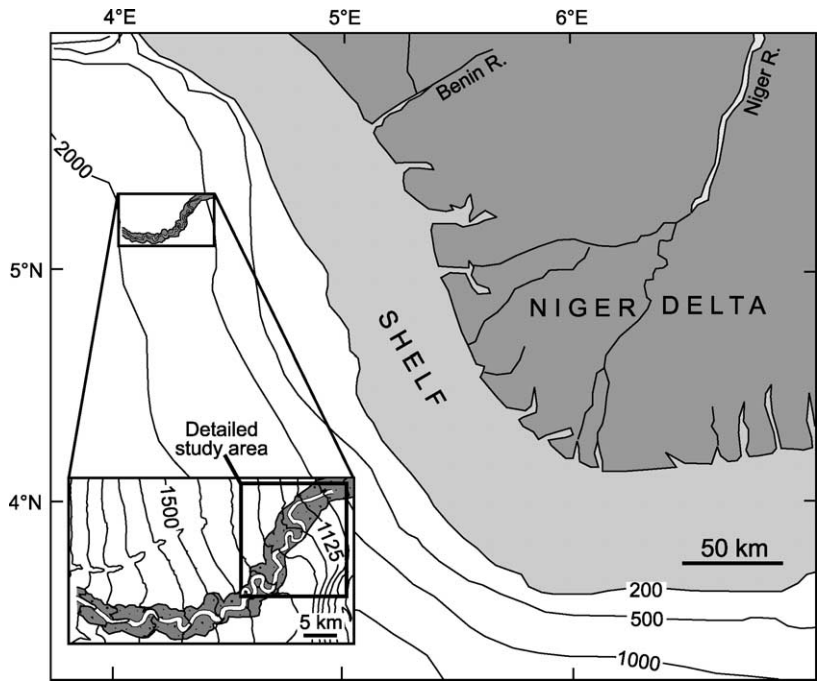

Fig. 6. Regional location map of Niger Delta, and the Benin-major channel-belt located on the western slope (inset shows close-up). Dark shaded zones represent locations dominated by inner levees and HARs. The sinuous white channel represents the final channel position prior to the abandonment of the system. The location of the smaller 3-D seismic sub-set (the detailed study area) is shown in the inset.

developed sediment waves that are most prominent near the outer bend of meander loops 1 and 3, where flow stripping is inferred to have been an important process (e.g. Fig. 8(c); see Piper & Normark, 1983; Normark, Piper, Posamentier, Pirmez, & Migeon, 2003).

The margins of the erosional fairway and outer levee crests are erosionally scalloped, as are the boundaries between successive periods of inner levee growth. A wide zone of D-C HARs is located just above the erosional fairway, near the base of the system, passing abruptly up-section into a narrower hybrid of D-C HARs and stacked channel-forms.

3.3. Evolution of the channel-belt

In the detailed study area (Fig. 7), the Benin-major CLS shows an evolution that can be divided into a period of incision followed by a three-phase fill history. Each fill phase is defined on the basis of planform channel geometry, channel-stacking architecture, and the nature of overbank deposits.

3.3.1. Incision

Prior to vertical incision of the Benin-major erosional fairway, erosional and depositional features associated with slope instability dominated the study area (Fig. 9(a)). Two parallel scarps, each about 20 m high, define a corridor through which slides passed over a failure plane (Fig. 7(a)). An arcuate shaped retrogressive failure scarp is observed west of the bathymetric high located at the southeastern corner of Fig. 7(a). Incoherent deposits accumulated above the failure plane at the base of the scarp. In most other areas, the failure plane appears to have been largely bypassed by mass wasted material. Several linear scours, some extending for greater than 10 km, are observed on the floor of the failure plane. Nissen, Haskell, Steiner, and Coterill (1999) interpreted these scours as glide tracks related to the passage of slide blocks. Posamentier, Meizarwin, Wisman, and Plawman (2000) provided an alternate explanation, interpreting similar features offshore eastern Kalimantan (Indonesia) as grooves that developed at the erosive base of large mass transport deposits. Both interpretations are consistent with a period of mass wasting.

In the northwestern corner of Fig. 7(a), two small leveed tributaries join the Benin-minor CLS. This much smaller system has a prominent erosive base that incises the same stratigraphic level as the failure scarps. The development of Benin-minor terminated during, or shortly after, prominent vertical incision of the Benin-major erosional fairway. The fairway erodes through a combination of parallel-bedded, in places polygonally faulted, strata inferred to correspond to mud-prone slope sediment, and chaotic units corresponding to mass transport deposits (Fig. 8).

A time-structure map of the erosional fairway at Benin-major reveals several important elements (Fig. 7(a)). The base of the erosional fairway consists of several cross-cutting, incised channels up to 350 m wide. They have a sinuous planform geometry, in some cases with sharp meander bends. One incised meander loop is terraced about 160 m above the thalweg of the erosional fairway, suggesting that channels had a sinuous planform geometry even during the earlier stages of incision (Fig. 7(a)). Several

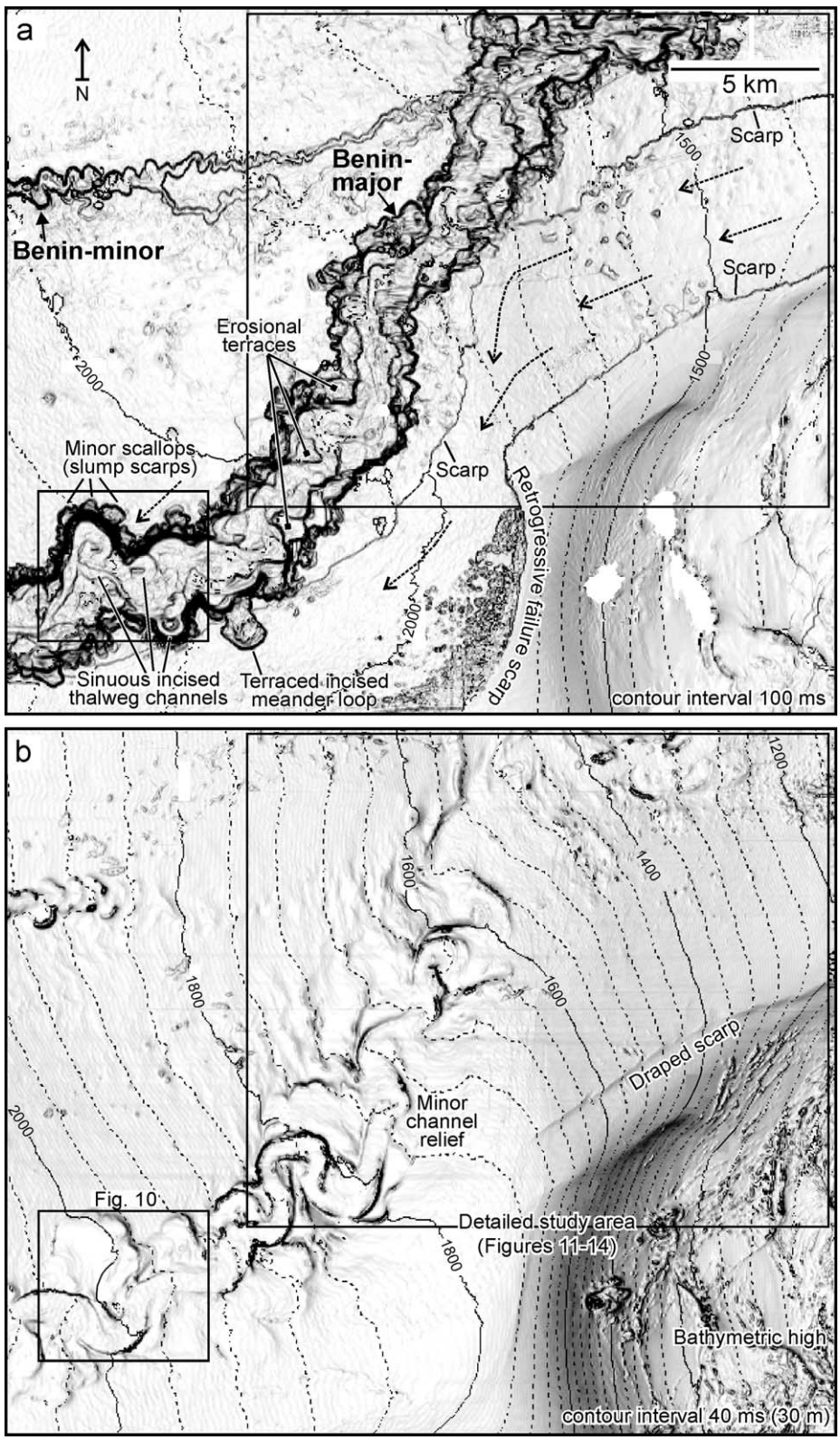

Fig. 7. (a) Contoured dip map from the erosive base of the Benin-major CLS, mapped along the base of the outer levees that flank the system. The surface represents a period of significant slope instability. The failure scarps define a corridor through which mass transport deposits passed. Dashed arrows indicate the orientation of linear scours believed to be related to the passage of mass transport deposits. Note the much smaller Benin-minor CLS (to the northeast) that incises the same surface that displays the failure scarps and linear scours. (b) Contoured dip map of the sea floor showing the modern day expression of the abandoned Benin-major CLS and surrounding area. Note that the failure scarps and the Benin-major CLS have little remaining relief. A single, sinuous channel is present along the axis of the Benin-major CLS.

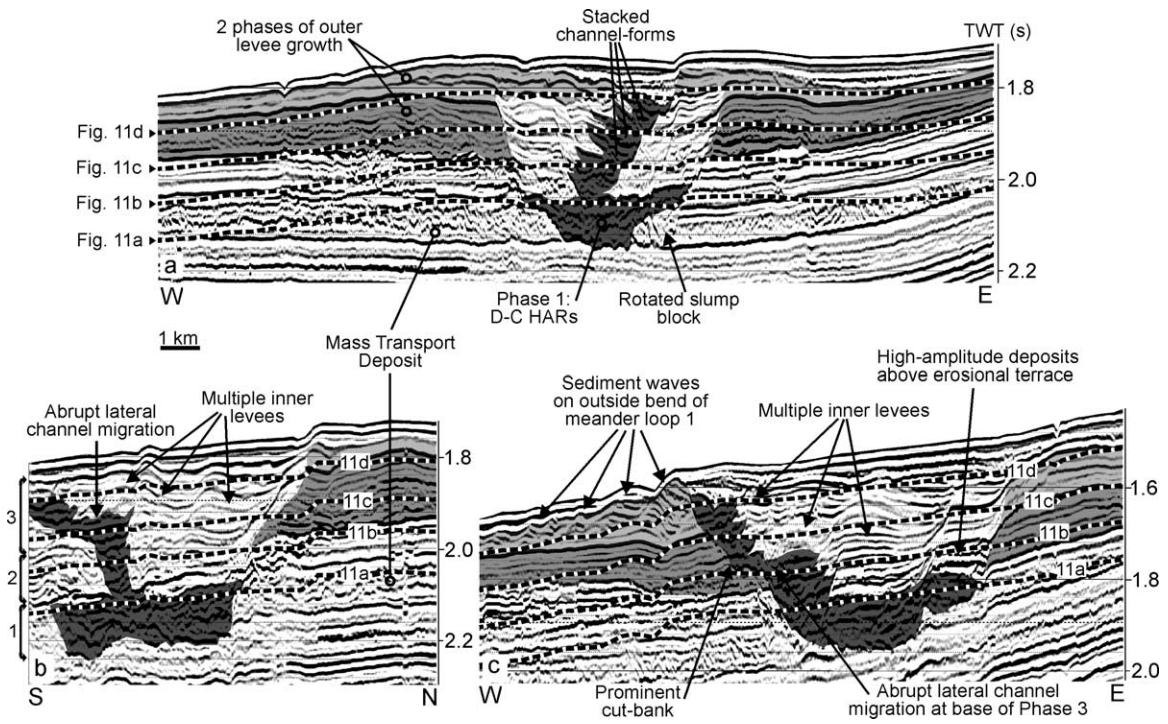

Fig. 8. Interpreted seismic profiles across Benin-major. (a) Profile roughly perpendicular to the axis of the erosional fairway, showing wide D-C HARs near the base of the system, and narrow HARs bordered by inner levees above. Narrow HARs migrates gently to the east (right) creating a cut-bank and a sharp transition between the channel deposits and inner levees. On the opposite side, an inter-fingering of channel deposits and inner levees is observed. Two phases of outer levee growth are recognized. (b) Interpreted profile perpendicular to the direction of meander loop 3, showing an increase in HAR width corresponding to an increase in lateral channel migration between 1920 and 1980 ms (middle of phase 3). Multiple phases of inner levee growth are recognized opposite the cut-bank. (c) Interpreted profile across migrating channel segment at meander loop 1, showing multiple phases of inner levee growth and a period of abrupt channel migration (base of phase 3). Rapid migration of this meander loop, therefore takes place at a deeper level than in the loop shown in Fig. 8(b). Locations shown in Fig. 12.

relatively horizontal erosional terraces, ranging in height from 20 to 100 m above the thalweg, are also recognized on the floor of the erosional fairway.

Scallops of various dimensions characterize the margins of the erosional fairway. The largest scallops probably originated from direct cut-bank erosion from incised sinuous channels at the base of the erosional fairway. Prominent incised meander bends on the floors of two large scallops in Fig. 10(a) support this interpretation. Some large and small scallops also originated from slumps that left behind curved slump scars. Rotational slump blocks, forming crescent-shaped inclined or flat benches, are observed adjacent to some scallops. Most are inferred to have formed during vertical incision (and hence destabilization) of the erosional fairway (see Friedmann, 2000; Pirmez, Beaubouef, Friedmann, & Mohrig 2000, Mayall & Stewart, 2000).

3.3.2. Fill—Phase 1

The interval directly above the floor of the erosional fairway is complex. It consists of a wide zone of D-C HARs with an overall tabular geometry, but also contains patches of low amplitude seismic facies, locally developed continuous HARs, and intact to semi-intact rotated slump blocks (Figs. 8, 9(c), 11(a) and 12).

In some areas, D-C HARs are located directly above the erosive base of the fairway; in other areas they are located above transparent to chaotic units interpreted as mass transport deposits (Fig. 10(d)). Horizon-slices indicate that D-C HARs consist of discontinuous remnants of sinuous channels that are largely confined within the deepest parts of the erosional fairway (Figs. 11(a) and 13(a)). A single channel cannot be mapped down the length of the system. The discontinuous channel remnants are inferred to originate from the self-cannibalizing nature of laterally migrating channels that underwent limited vertical aggradation. Cross-sections indicate that periods of cut-and-fill were common within the phase 1 fill, sometimes resulting in the development of erosional terraces. Continuous very high amplitude seismic reflections and/or low amplitude inner levee deposits overlie some erosional terraces (e.g. Fig. 10). Patches of low amplitude seismic facies within the phase 1 fill may be the remnants of mass transport deposits, dissected during periods of channel re-incision, or the remnants of early inner levees. Such mud-prone deposits act as baffles to the flow of hydrocarbons, and are therefore an important consideration when assessing the reservoir performance of the phase 1 fill.

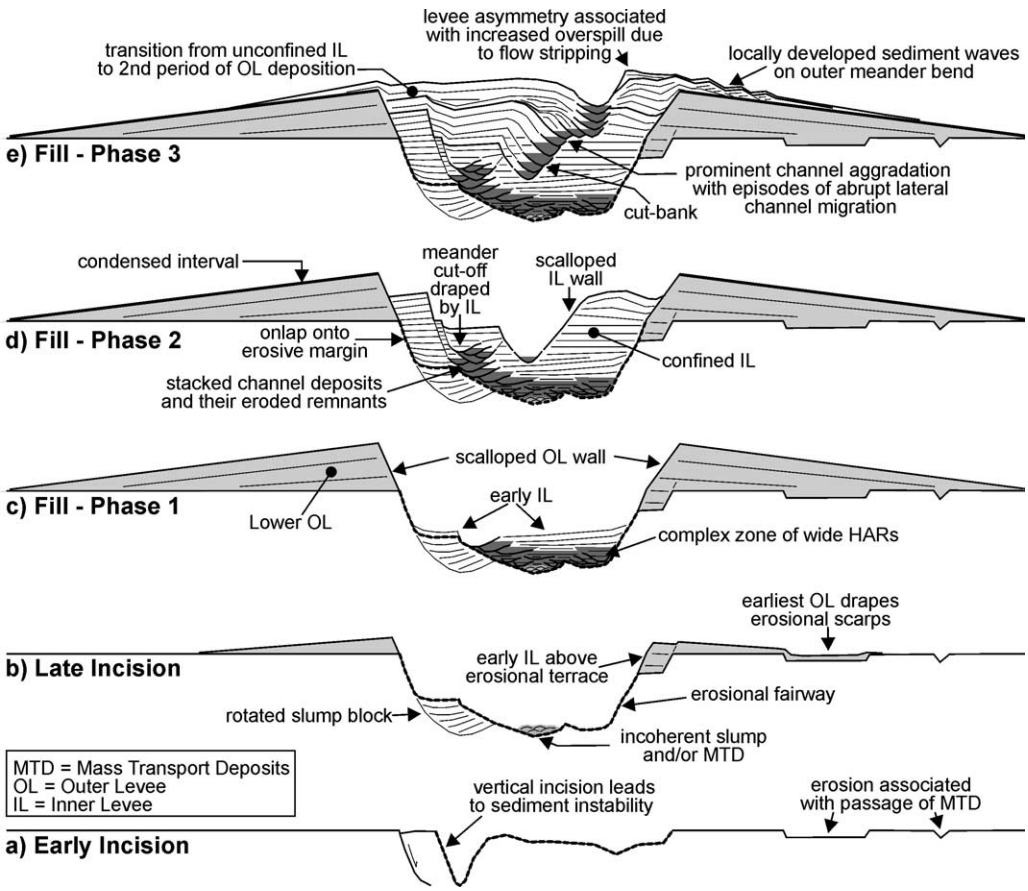

Fig. 9. Generalized schematic drawing showing the incision (a–b) and three-phase fill history (c–e) of the Benin-major channel-levee system. See text for details.

3.3.3. Fill—Phase 2

Phase 2 is characterized by a period of prominent vertical inner levee aggradation that outpaced channel floor aggradation. The base of phase 2 is defined by the first (deepest) channel that can be mapped down the entire 23 km long segment within the primary study area (Figs. 9(d) and 13(a)). During phase 2, the planform channel geometry exhibits a tortuous sinuosity (average of 1.63, and a range of 1.47–1.80), with immature meander loops that have a short radius of curvature and short wavelengths (Figs. 13(a)). Phase 2 HARs are narrower than phase 1 HARs, and consist of a combination of stacked channel-forms and D-C HARs. Along some channel segments, eroded remnants of channel-forms are observed where they have been incised by an adjacent or overlying one.

Horizon-slices through phase 2 channel-axis deposits show sporadic changes in the number of channel bends and in sinuosity. These changes can be abrupt, the result of meander cut-offs, or subtle, the result of slight changes in the thalweg path, with some channel reaches shifting from slightly sinuous to straight, and vice versa (Fig. 13). Two meander cut-offs are observed, each results in a decrease in the number of channel bends and a corresponding decrease in sinuosity (Figs. 11(b) and 13(b)). Both cut-offs were later draped by inner levees (e.g. Fig. 11(c)).

The most pronounced inner levees appear to have developed during phase 2. Inner levee ‘terraces’ were at a maximum height above the channel thalweg, onlapping and to some extent stabilizing, the scalloped margins of the erosional fairway. Sharp, erosive channel walls were located on one or both sides of the narrow channel-axis. In some areas, minor scallops along the channel walls are interpreted as slump scarps formed when sediment from the inner levees failed into the channel-axis. In other locations, minor scallops along the margins of the erosional fairway developed as sediment was shed from the outer levee and erosional fairway walls and accumulated above inner levee ‘terraces’ (e.g. Figs. 7(a) and 10). In Fig. 10, for example, two minor scallops are observed along the margin of the system. A subtle thickening within the adjacent inner levee (Fig. 10(d)) is interpreted as the corresponding slump deposit (Fig. 10(e)).

The cross-sectional and planform geometry of the system during phase 2 is inferred to have resembled that of the modern ‘empty’ terraced upper fan channel-belts on the Zaire (Droz et al., 1996) and Indus fans (Von Rad & Tahir, 1997; Fig. 15).

3.3.4. Transition—Phase 2 to Phase 3

The planform channel geometry established in phase 2 transforms abruptly into a much different channel planform

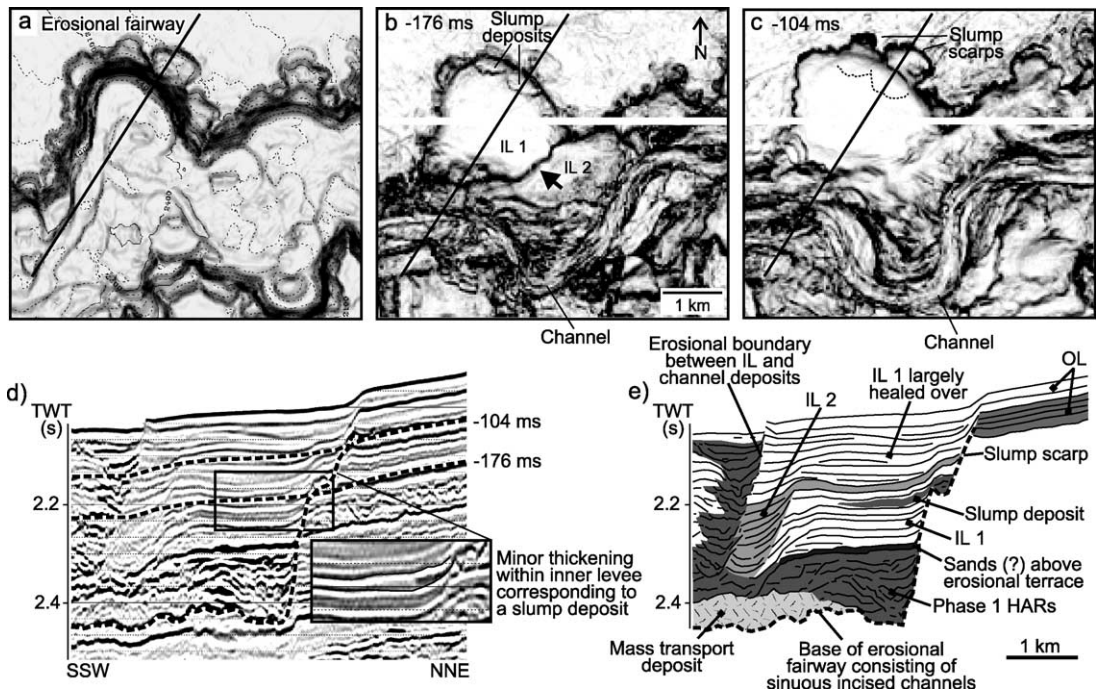

Fig. 10. (a) Dip map of the base of incision of the erosional fairway at Benin-major. Note the two incised meander loops located at the base of the prominent scallops. The large arcuate scallops are interpreted to have formed from cut-bank erosion (probably accompanied by slumping) associated with the incised sinuous channel. The smaller scallops are interpreted as slump scarps that developed sometime after the initial incision of the erosional fairway. (b) Dissemblance horizon-slice at 176 ms below the sea floor showing potential slump deposits within inner levee 1 (IL 1), suggesting that the smaller-scale scallops developed after inner levee deposition had begun. (c) Dissemblance horizon slice at 104 ms below the sea floor crossing channel and inner levee deposits, and also crossing the smaller-scale scallops. (d) Seismic profile and corresponding line drawing (e) across the northern margins of the system. Two major periods of inner levee growth are recognized as well as a slight thickening within IL 1, corresponding to the interpreted slump deposit associated with the smaller-scale scallop (also crossed by the profile). The boundary between the first and second inner levees is sharply defined in (b) (arrow), whereas it is barely discernible in (c) where the horizon slice no longer crosses the boundary between two inner levees. Location shown in Fig. 7.

geometry by phase 3. The transition from phase 2 to phase 3 is abrupt, marked by a decrease in the number of channel bends. The planform geometry evolves rapidly from a tortuous geometry with 18 channel bends (at 224 ms below sea floor), to a much straighter geometry with 11 channel bends (at 192 ms below sea floor—Fig. 13(b)). Planform channel re-adjustments create a 'rope-like' fabric on dissemblance slices.

Although the overall sinuosity decreased as the channel-axis straightened, several meander loops maintained their form during the transition to phase 3 (e.g. loops 1, 2, 3 and 4—Fig. 12). In fact, loops 1 and 2 show an abrupt increase in their radius of curvature, with a corresponding abrupt shift in the channel position at the bend, opposite to the trend observed elsewhere (Fig. 12). The period of accelerated channel migration is expressed in cross section as a localized lateral offset in the HARs (Fig. 8(c)).

3.3.5. Fill—Phase 3

In comparison to phases 1 and 2, the overall channel floor aggradation rate increased during phase 3 (relative to the inner levee aggradation rate). Phase 3 begins at 192 ms below the sea floor, with an abrupt increase from 11 to 14 channel bends in the lowermost 24 ms, above which the system shows a consistent number of channel bends (14) through its remaining history. Although the number of channel bends remains constant, the planform geometry of the stacked channel-forms evolves during aggradation (Figs. 9(e) and 13(a)). Phase 3 is characterized by narrow channel-forms that stack near vertically, locally showing abrupt lateral offset (migration) and incision between channel-forms. Successive channel-forms commonly migrate both in the down-channel (sweep) and cross-channel (swing) direction, with only one meander loop showing a component of up-dip migration (loop 4—Fig. 12).

There is a consistent increase in sinuosity through time, from 1.65 at the base of phase 3 to a maximum of 2.07 near the top (average 1.9). Near the middle of phase 3, a period of accelerated meander growth rate occurred (similar to the transition from phase 2–3 in loops 1 and 2). This is particularly evident at meander loops 2 and 3, which show a dramatic increase in the radius of curvature as the channel-axis migrated laterally, eroding rapidly into the cut-bank (Fig. 12). A vertical profile perpendicular to the direction of channel migration on meander loop 3 shows an increase in the width of the HARs, and multiple phases of inner levee growth opposite to the cut-bank, occupying former channel positions (Fig. 8(b)). On dissemblance horizon-slices, older channel positions (now occupied by inner levees) are

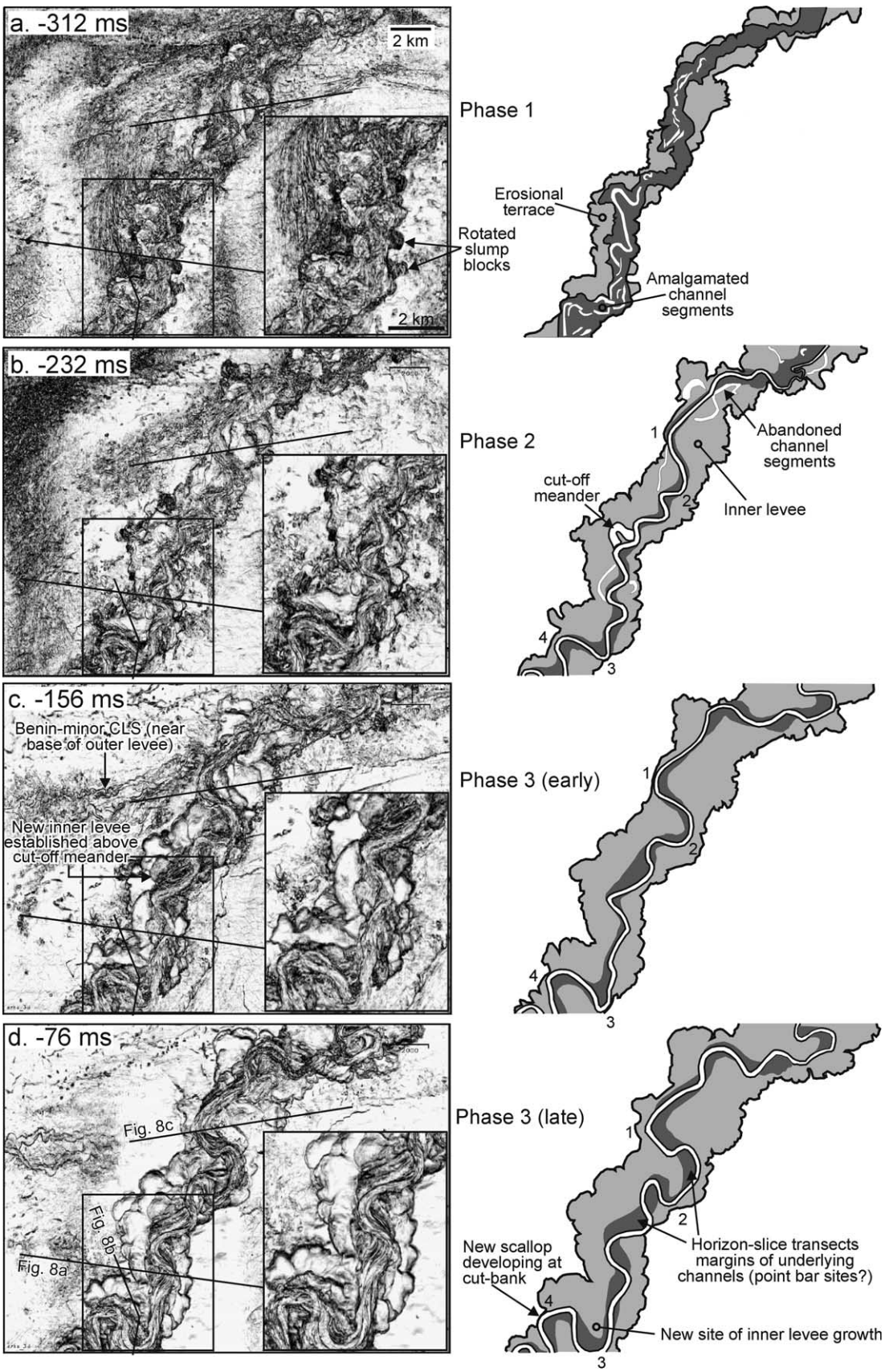

Fig. 11. Series of uninterpreted dissemblance horizon-slices, flattened on the seafloor with corresponding line drawings at (a) 312 ms (phase 1), (b) 232 ms (phase 2), (c) 156 ms (phase 3), and (d) 76 ms (phase 3) below the sea floor. See text for details.

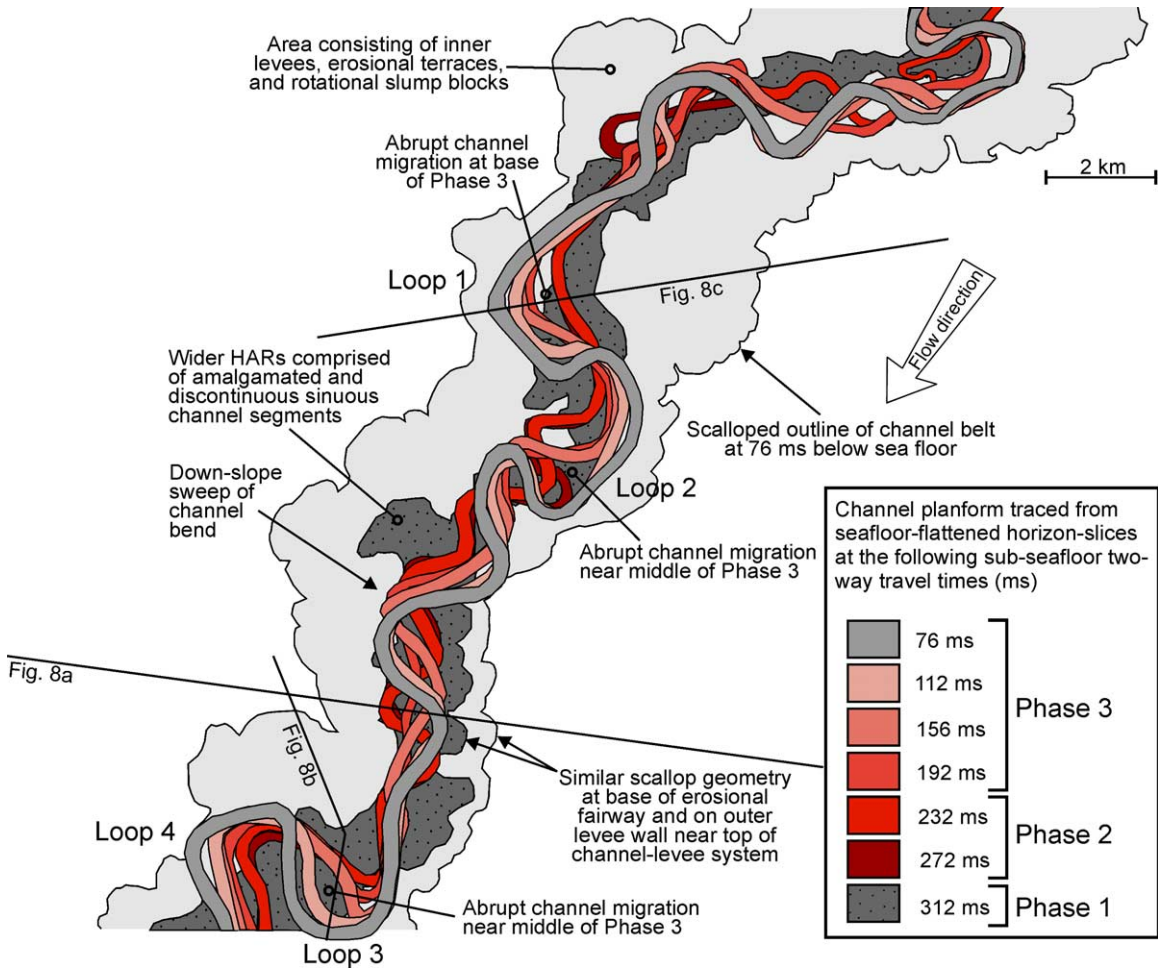

Fig. 12. Drawing showing the planform geometry of the stacked channel-axis deposits (HARs) every 36 to 40 ms below the sea floor (from seafloor-flattened dissemblance slices). Note the overall down-channel migration and the abrupt jumps at some meander loops where abrupt channel-migration has taken place. Channel-axis deposits aggrade and migrate within the scalloped confines of the erosional fairway, where inner levees flank the phase 2 and phase 3 channel deposits.

observed on the inside bend of meander loop 3 (Figs. 11(d) and 14). It is unclear whether this inner bend formed as a result of lateral accretion (similar to the Lateral Accretion Packages described by Abreu et al., 2003), or whether the inner bend formed as a result of multiple periods cut-and-fill, with channels migrating into a cut-bank (e.g. as in Fig. 5(b)). The limitations of seismic resolution in this case preclude distinguishing between the two.

The average sinuosity increased at a slower rate (relative to aggradation) near the top of phase 3, and eventually decreased as the system was abandoned (Fig. 13(b)). Because channel floor deposits aggraded at a faster rate than the inner or outer levees, there was a progressive decrease in channel relief during phase 3. The final channel had very little relief, and thus if a particularly large flow had traversed the channel, it probably would not have been contained between the levee crests, and may have lead to an avulsion. The final abandonment of the Benin-major CLS occurred when a mass transport deposit, originating from the east, was deposited above the southeastern upper outer levee. The mass transport deposit has a maximum thickness of about 60 m, and appears to have plugged the remaining depositional relief of the youngest channel in the detailed study area (which prior to the mass transport deposit had a depth between 50 and 75 m).

3.4. Outer levee deposition

The erosional scarps, linear scours, and the Benin-minor CLS, were all draped by the lower outer levees of Benin-major. Determining the precise timing for the start of outer levee deposition, however, is difficult. Three lines of evidence help to constrain it. First, some scallops observed along the margins of the erosional fairway (e.g. at −312 ms in Fig. 11(a)) have the same geometry as much shallower scallops developed along the margins of the lower outer levee walls (e.g. at −76 ms in Fig. 11(d)). The same scallop geometry, extending from the incision near the base of the erosional fairway, up to near the top of the lower outer levee walls, implies that outer levee deposition began during the incision of the erosional fairway or the phase 1 fill (Fig. 12).

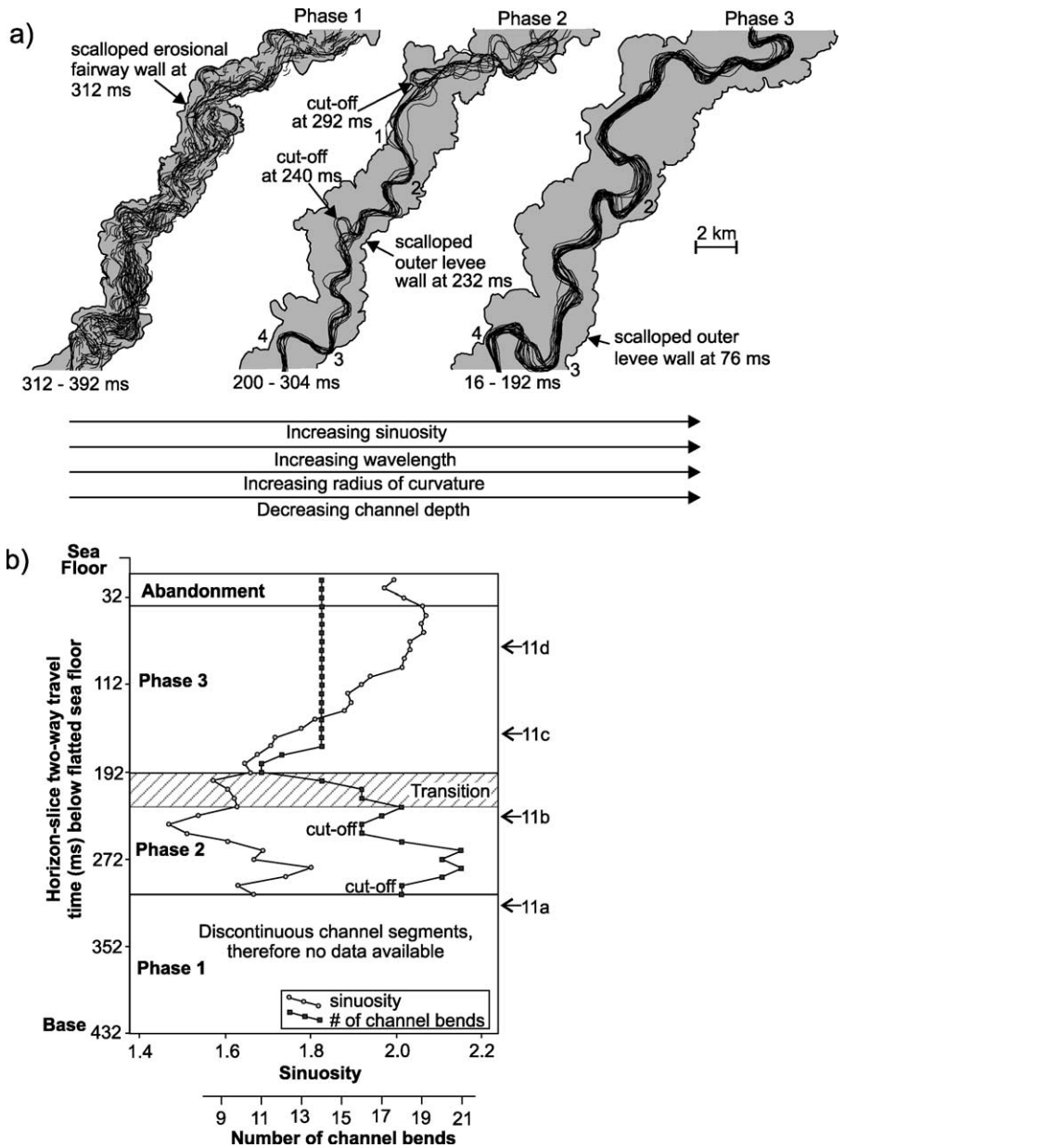

Fig. 13. (a) Channel-centerline plots every 8 ms showing three phases of channel deposit evolution at Benin-major. *Phase 1* corresponds to the wide zone of HARs deposited within the erosional fairway and is inferred to consist of amalgamated channel segments and slump deposits (originating from failures along the erosional fairway and/or outer levee walls). Channel paths show little vertical aggradation and are self-cannibalizing with significant lateral migration, resulting in a tabular zone of HARs. *Phase 2* corresponds to channel geometries displaying a tortuous sinuosity, with immature meander loops that have a short radius of curvature and wavelength. The number of meander bends and sinuosity change sporadically due to subtle changes in the thalweg path and meander cut-offs. The transition from phase 2 to phase 3 occurs abruptly as the channel goes through a period of straightening. *Phase 3* begins when the channel-planform geometry has stabilized, with a consistent number of meander bends and an overall increase in sinuosity, from about 1.65 to 2.07. Phase 3 channel deposits show a progressive increase in meander wavelength, radius of curvature, and channel-floor aggradation rates (relative to inner levees), and ends when the system is abandoned. (b) Chart showing vertical trends in the number of channel bends and sinuosity, from the base of Benin-major to the modern sea floor. Note the meander cut-offs corresponding to decreases in sinuosity in phase 2 and the abrupt decrease in the number of channel bends during the transition to phase 3. The location of horizon slices in Fig. 11 are shown on the left.

Second, inner levees associated with the phase 2 fill, onlap the outer levee walls, requiring the outer levees to have formed earlier. Third, on some profiles outer levees drape erosional terraces along the margins of the erosional fairway, implying that the outer levees developed sometime after the earliest incision (e.g. the terraced meander loop in Fig. 7(a) is draped by outer levee deposits). The lower outer levees, therefore, appear to have been deposited sometime after the start of vertical incision, but before the phase 2 fill (Figs. 9(b) and (c)).

4. Discussion

4.1. Origin of 'terrace' forming elements

An inspection of the literature indicates that terrace-like features are recognized in a wide range of CLSs, including those within large fans like Zaire (Droz et al., 1996; Vittori et al., 2000), Indus (Von Rad & Tahir, 1997), Bengal (Hubscher et al., 1997), Toyama (Nakajima et al., 1998), and Laurentian (D. Piper, pers comm. 2002), medium-sized fans like Rhone (Bellaiche et al., 1984; Torres et al., 1997) and Monterey (Garner, Bohannon, Field, & Masson, 1996), and smaller fans like Hueneme (Piper et al., 1999), North and South Golo (Pichevin, 2000), and Einstein (Hackbarth and Shew, 1994; C. Winker, pers comm. 2001).

Interpretations for the origin of terraces vary widely, from levee margin growth faults (Clark and Pickering, 1996), slumped levee material (Hackbarth & Shew, 1994) and rotated slump blocks (originating from channel walls—Shepard & Emery, 1973; Kenyon et al., 1995; Friedmann, 2000), to depositional terraces (Von Rad & Tahir, 1997), channel-bank deposits (McHargue & Webb, 1986; Kolla & Coumes, 1987), confined or underfit inner levees (Hubscher et al., 1997; Torres et al., 1997; Piper et al., 1999), to rejuvenation features resulting from channel entrenchment into flat-lying strata (i.e. erosional terraces—Normark, 1978; O'Connell, McHugh, & Ryan, 1995).

Three different types of terrace-forming elements are recognized in the channel-belts examined in this study: rotated/subsided slump blocks, erosional terraces, and inner levees. The relative importance of each terrace-type varies from one system to another, and during different periods in the evolution of each system.

Several intact and semi-intact slump blocks are recognized locally along the margins of the erosional fairways at Benin-major and Indus Fan (Figs. 4c, 8(a) and 11(a)). In some cases they contain seismic markers that can be correlated to undeformed strata adjacent to the system. Most slump blocks developed during the incision of the erosional fairway, or during its early fill history, when its margins were most unstable. Slump block movement is accommodated both by rotation along listric fault planes and subsidence into underlying poorly consolidated strata. At Benin-major, slump blocks are commonly sculpted along their channel-ward-exposed surfaces by channels associated with the phase 1 HARs.

Purely erosional terraces are also recognized locally along the margins of erosional fairways in both study areas (e.g. Figs. 2 and 3). Many erosional terraces formed during the incision of the erosional fairway. They form flat benches consisting internally of strata deposited prior to the incision of the erosional fairway. At Benin-major, erosional terraces are also recognized within the phase 1 deposits where they are associated with rejuvenated incision, and in phase 2 deposits where they are associated with meander loop cut-offs (e.g. Fig. 11(b)).

Both slump blocks and erosional terraces (remnants and cut-offs) commonly become sites of prominent inner levee deposition (e.g. Figs. 2, 3, 9(c)–(d) and 14). Inner levees, which also develop independent of pre-existing terrace relief, are commonly found adjacent to narrow HARs and onlap the outer levee and erosional fairway walls. At least three periods of inner levee growth are recognized in both study areas (e.g. Figs. 4(b), 8(b) and (c)). They are best preserved opposite major cut-banks, where the channel-axis has consistently migrated away from one channel wall and towards another. For example, as the channel-axis migrated towards the outer levees in Figs. 4(b) (CLS C2) and 8(c) (Benin-major), several phases of inner levee growth occupied former channel positions opposite the prominent cut-bank. Each successive period of inner levee growth onlaps and/or drapes the previous one, creating a 'stepped' channel margin profile. Multiple inner levee 'steps' may aggrade at different levels above the channel floor at the same time, and probably at different rates. The inner levee closest to the channel-axis appears to aggrade at the fastest rate.

Inner levee terraces merge with outer levee crests when the rate of inner levee growth exceeds that of the outer levees, leading eventually to the 'healing' of the terrace relief. At Benin-major, deposition resumed above the lower outer levee once the inner levees aggraded near the level of the lower outer levee crests. As this occurred, the confined inner levees evolved into unconfined inner levees and eventually back into outer levees. The result was a shift in the outer levee crests towards the axis of the under-fit channel (e.g. Fig. 8(a), see also Skene, 1998).

Cross-sectional profiles in both study areas show that between 45 and 60% of the channel-belt consists of inner levees.

4.2. Lithological composition of inner levees

The acoustic character of inner levees in both study areas ranges from low amplitude and almost transparent, to moderate amplitude and well stratified. Their acoustic character can be in striking contrast to adjacent outer levees (e.g. Fig. 3), suggesting that they can be compositionally different. The near-transparent character of some inner levees implies a uniform lithological composition. Shallow piston cores obtained from inner levees on other fans indicate that they are mud-prone (e.g. Von Rad & Tahir, 1997; Hubscher et al., 1997), but these studies only sampled the uppermost parts of inner levees.

HARs, resembling C-P HARs, are observed locally within inner levees (e.g. Fig. 4(c)) or above other elevated regions of the channel-belt (e.g. erosional terraces or meander cut-offs—Figs. 5(c) and 10(d)). These HARs are interpreted as sand-prone sheet-like or pod-like deposits, although the mechanism for their formation is poorly understood. Clark and Pickering (1996) inferred that sandy deposits could form above channel terraces or benches as

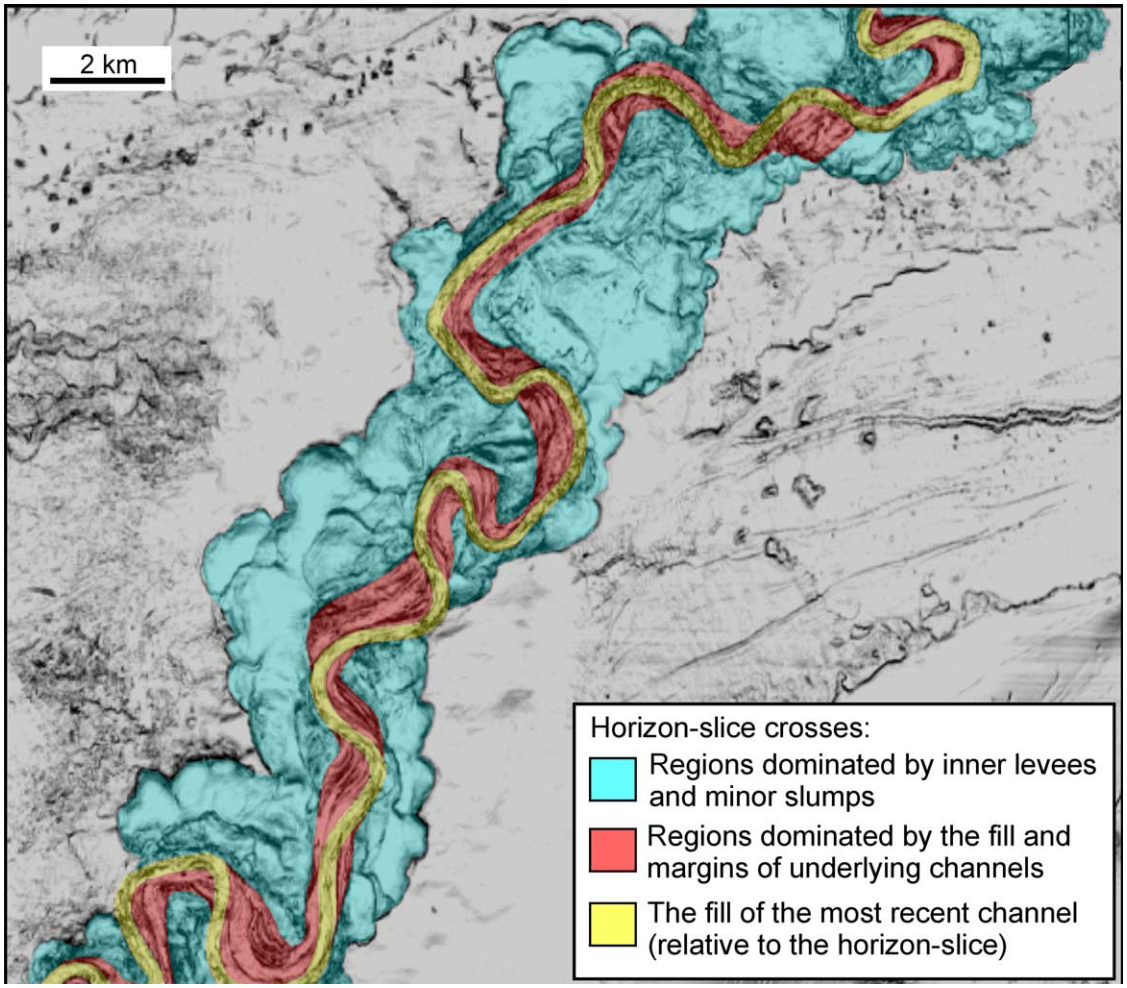

Fig. 14. Dissemblance horizon-slice at 76 ms below the flattened sea floor horizon. The horizon-slice crosses the stacked channel-forms that occupied the system during phase 3 (yellow and red) as well as inner levee dominated facies that developed during phases 2 and 3 (blue).

a result of hydraulic jumps within the through-channel turbidity current. Piper et al. (1999) documented sandy deposits, forming beds a few meters thick, interbedded with muddy inner levee sediment in the Hueneme fan valley (CLS), in the Santa Monica Basin, offshore California. In addition, cores from Site 934 on Amazon Fan (ODP Leg 155) demonstrate that an inner levee, deposited above a meander cut-off on the most recently active Amazon Channel, consists of thick muddy turbidites (up to 30 cm thick—Piper & Deptuck, 1997) interbedded with fine-grained sands. Inner levees may also contain slump deposits shed from the outer levee or erosional fairway walls, as observed in Fig. 10.

Too few inner levees, however, have been calibrated with cores, and consequently there is considerable uncertainty about their composition and whether there are systematic changes in lithology from bottom to top or from one system to another. There is also uncertainty whether different types of inner levees (e.g. those formed as a result of under-fit confined flows versus those developed above meander cut-offs) are compositionally different. Whether inner levees are mud-dominated, or contain significant sandy intervals, has important implications for potential reservoir communication with adjacent sinuous channels, and therefore warrants further study.

4.3. HARs—Indus Fan and Benin-major

HARs show significant variability in width, acoustic character and vertical stacking patterns in both study areas. Variations in width can be real, or can reflect the orientation of the seismic profile relative to the orientation of the channel-axis. Since the orientation of the channel-axis can evolve through time, a single vertical seismic profile may show apparent variations in width that do not necessarily reflect changes in the channel width through time. In addition, the ratio of channel aggradation to channel migration may also influence the horizontal extent of HARs. Narrow channels that stack vertically will produce narrow HARs; narrow channels that stack adjacent to one another (i.e. laterally), with little vertical aggradation, will produce wider HARs.

On the Indus Fan, HARs can be as much as 800 m thick and show a complex ‘multi-limb’ or ‘branching-cactus’

aggradational pattern in cross-section (e.g. Figs. 2–4). In the Benin-major CLS, the cross-sectional character of HARs is less complex than on the Indus Fan. The base of the system consists of a wider zone of HARs (confined within the erosional fairway) that passes up-section into one or more aggradational 'limbs' of narrow HARs (the number of 'limbs' depends on whether a meander loop or a straight channel segment is crossed). In general, the CLSs in both study areas contain HARs that are wider near the base (within the erosional fairway) than they are near the top.

Cross-sectional profiles in both study areas show that between 40 and 55% of the channel-belt consists of HARs. The fill of the basal erosional fairway, on the other hand, may consist of greater than 75% HARs, with the remainder consisting of transparent seismic facies interpreted as early inner levees and/or muddy slump deposits shed from channel walls.

4.4. Relationship between channel migration and inner levee deposition

The aggradation of channel deposits at Benin-major records both down-channel and cross-channel migrations (see also Posamentier et al., 2000; Abreu et al., 2003). The Benin-major CLS demonstrates that some channels adjust their planform geometry periodically, perhaps in response to changes in the equilibrium profile or flow character (e.g. size, composition). In addition, different parts of the same channel may evolve in different ways. A single meander loop can undergo a period of rapid lateral migration at the same time that other segments of the same channel show little migration (see also Kolla, Bourges, Urruty, & Safa, 2001).

The history of inner levee deposition is intimately linked to the evolution of channels. On horizon slices (both amplitude and dissemblance), major periods of inner levee growth are separated by sharp boundaries (e.g. Fig. 10(b)) that are sometimes erosionally scalloped (e.g. Figs. 11(c) and 14). The development of distinct boundaries between inner levees implies that the channel-axis migrated in discrete pulses, eroding into the cut-bank, and creating space for a new inner levee to develop. The scalloped margin of the inner levee is preserved as it is onlapped and draped by the adjacent, younger inner levee (Figs. 8(b) and (c)). After a period of rapid channel migration and new inner levee growth, channel position is inferred to be relatively stable, characterized by vertical channel-fill and inner levee aggradation, with gradual, rather than abrupt, lateral channel migration.

The trigger for abrupt lateral channel migrations is poorly understood. Kolla et al. (2001) postulated that periods of discrete channel migrations were the result of stronger, surge-type flows, whereas periods of gradual channel migration and vertical aggradation were the result of steady-type flows. At least two mechanisms can promote the rapid lateral migration of channels. Episodic failure of the outer bend of a meander loop (via a slump) can promote a rapid lateral shift in the channel by removing the confining channel wall. Such failures could be triggered by the undercutting of the channel wall at a cut-bank during the passage of surge- or steady-type flows, or even by tectonism, unrelated to the passage of a flow.

Abrupt deposition of a debrite plug could also promote rapid channel migration by changing the gradient profile along the channel. On a straight channel segment, the channel may respond by incising the plug to re-establish an equilibrium gradient profile. On a meander bend, however, the plug may promote accelerated cut-bank erosion, leading to a period of rapid channel migration, or may promote erosion at the neck of a meander loop resulting in a cut-off. A contorted slump deposit at Site 934 on the Amazon Fan, for example, is believed to have triggered a meander cut-off on the most recently active channel (Flood, Piper, & Shipboard Scientific Party, 1995). The slump may have partially filled the channel, causing flows to divert around it and across the narrow meander neck. The alternative hypothesis was that the emplacement of an underlying 18 m thick sand unit plugged the channel, in turn causing the undercutting of the channel banks, leading to the failure of the levee margin (Flood et al., 1995).

4.5. Scaled comparisons with other systems

Regardless of whether a CLS is isolated (as in Benin-major) or whether several systems stack adjacent to one another (as in CLC C on Indus Fan), individual CLSs in both study areas are characterized by a basal erosional fairway flanked by outer levees, containing under-fit channels flanked by inner levees. Similar architectural styles are repeated at multiple scales in upper fan CLSs around the world, including several other systems on the Niger Delta slope (e.g. Benin-minor) and in the Arabian Sea (e.g. modern Indus Fan), as well as CLSs on the modern Zaire (offshore Angola), Bengal (offshore India and Bangladesh) and Rhone (Mediterranean Sea) fans (Fig. 15). At least two CLSs in the eastern Gulf of Mexico also show similar architectural styles; they include the very small Einstein CLS (Hackbarth & Shew, 1994) and the larger Joshua CLS (Posamentier, 2003). All of these systems are floored by erosional fairways with incision ranging from a few tens to a few hundreds of meters, and are bordered by outer levees that vary significantly in thickness (at their crest—from one system to another). Together they confine channel-belts that vary over an order of magnitude in width, from 1 km (e.g. Benin-minor) to greater than 10 km (e.g. modern Indus—see Fig. 15). The channel-belts commonly contain sinuous channels that vary in width from less than 100 m to greater than 1 km, and show strong evidence for inner levee development with heights above the channel-floor ranging from less than 20 m to greater than 360 m.

We also recognize similar architectural styles in some systems that have much shorter length-scales, that feed

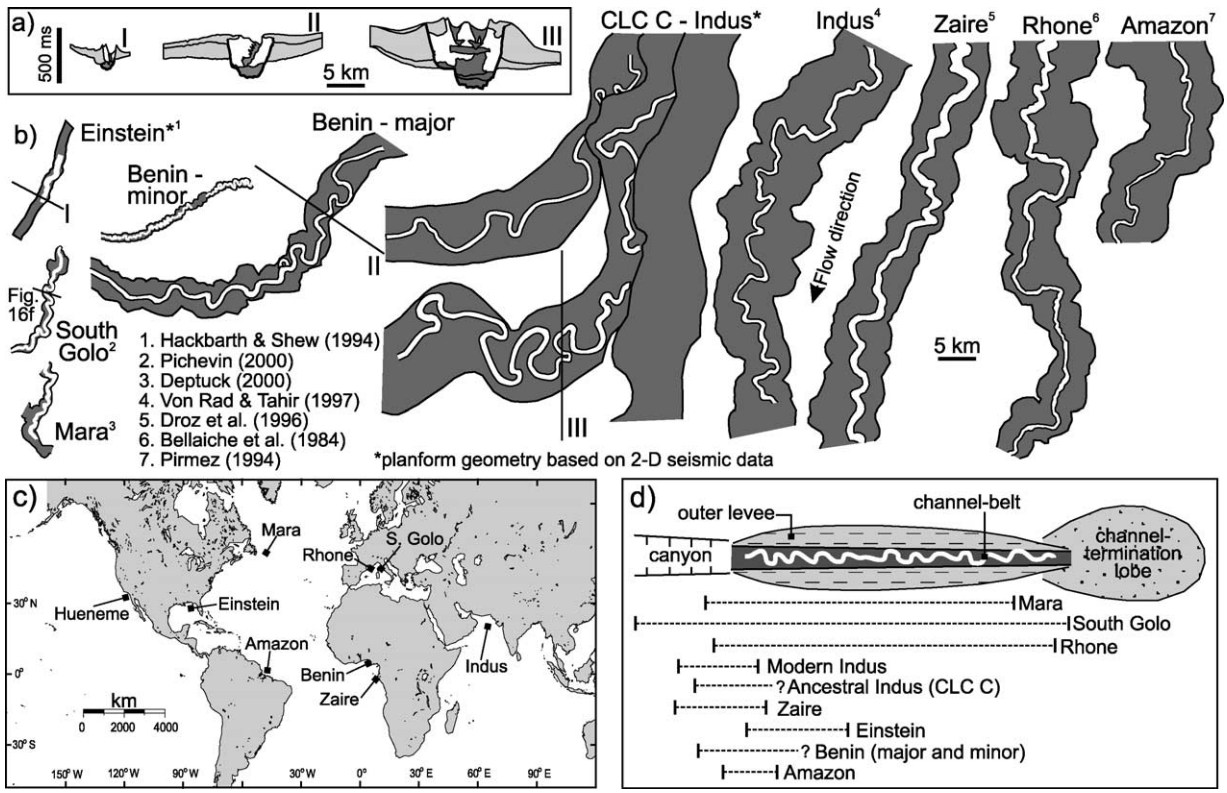

Fig. 15. (a) Scaled comparison of three cross-sections through channel-levee systems, showing the range of dimensions from small systems like Einstein (Gulf of Mexico), to very large systems like CLS C2 on the Indus Fan. All three examples consist of the same types and similar configurations of architectural elements (erosional fairway, inner levees, outer levees, channel-axis deposits), with significant variability in scale. (b) Scaled comparison of selected channel-belt planforms, from small systems like South Golo (offshore east Corsican margin) and Einstein (Gulf of Mexico), to large systems like the modern Indus, Zaire, Amazon and Rhone. Only the upper fan portions of the channel-belts are shown, although in most cases data exist down-slope (e.g. Zaire). It is noteworthy that the planform channel-axis geometry shown for the modern Indus, Zaire, Rhone, Amazon, and South Golo represent the modern erosive channel-thalweg within an unfilled CLS, whereas the planform channel geometry shown for Indus CLSs C1, C2 and the Benin-major CLS represents the final channel position prior to the abandonment of each system, mapped from HARs (channel deposits). (c) The approximate locations for systems shown is (b). (d) Simplified schematic diagram of a CLS showing the length and extent of coverage of each channel-belt shown in (b), relative to the entire length of the system. Note that nearly the entire length of S. Golo, Mara, and Rhone are shown, whereas only the upper fan reaches of Indus, Zaire, Amazon, Benin, and Einstein are shown.

small fan systems deposited in relatively confined basins, like Hueneme (offshore California—Piper et al., 1999), South Golo (offshore eastern Corsica—Pichevin, 2000), and Mara (early Paleogene Jeanne d'Arc Basin, eastern Canada—Deptuck, 2000). The South Golo CLS, for example, was mapped using ultra-high frequency Huntec DTS seismic data (<1 m vertical resolution). The system formed off the mountainous eastern margin of Corsica, along the edge of a narrow (25 km wide) and relatively shallow (<900 m deep) trough-shaped basin. The South Golo CLS is much smaller and shorter than Benin-major (a mapped length of about 18 km—Fig. 15(a)), but shows the same architectural elements with configurations similar to the mush larger systems described in this paper. Although data quality is not sufficient to identify individual channel-forms, a channel-belt consisting of HARs and inner levees is well imaged (see also Pichevin, 2000). In Fig. 16(f), the channel-axis deposits (expressed as HARs) were generated from a sinuous channel that migrated to the left during aggradation, creating a prominent cut-bank and multiple periods of inner levee growth opposite the cut-bank.

The recognition of similar architectural elements, in systems that vary significantly in size and setting, suggests that common channelized flow processes exist at different scales. There also appear to be general evolutionary trends in many upper fan CLSs that lead to common architectural configurations.

4.6. Linking seismic- and outcrop-scale observations

Relating the architectural styles described above to outcrops can be challenging. This is due largely to differences in resolution between outcrop and seismic data, and limited well control to bridge the resolution gap. In addition, outcrops are rarely laterally extensive enough to allow for a broad-scale perspective or vertically extensive enough to expose the base and top of most CLSs (a problem that is also encountered in high-resolution seismic studies). Perhaps the most important consideration is aspect ratio.

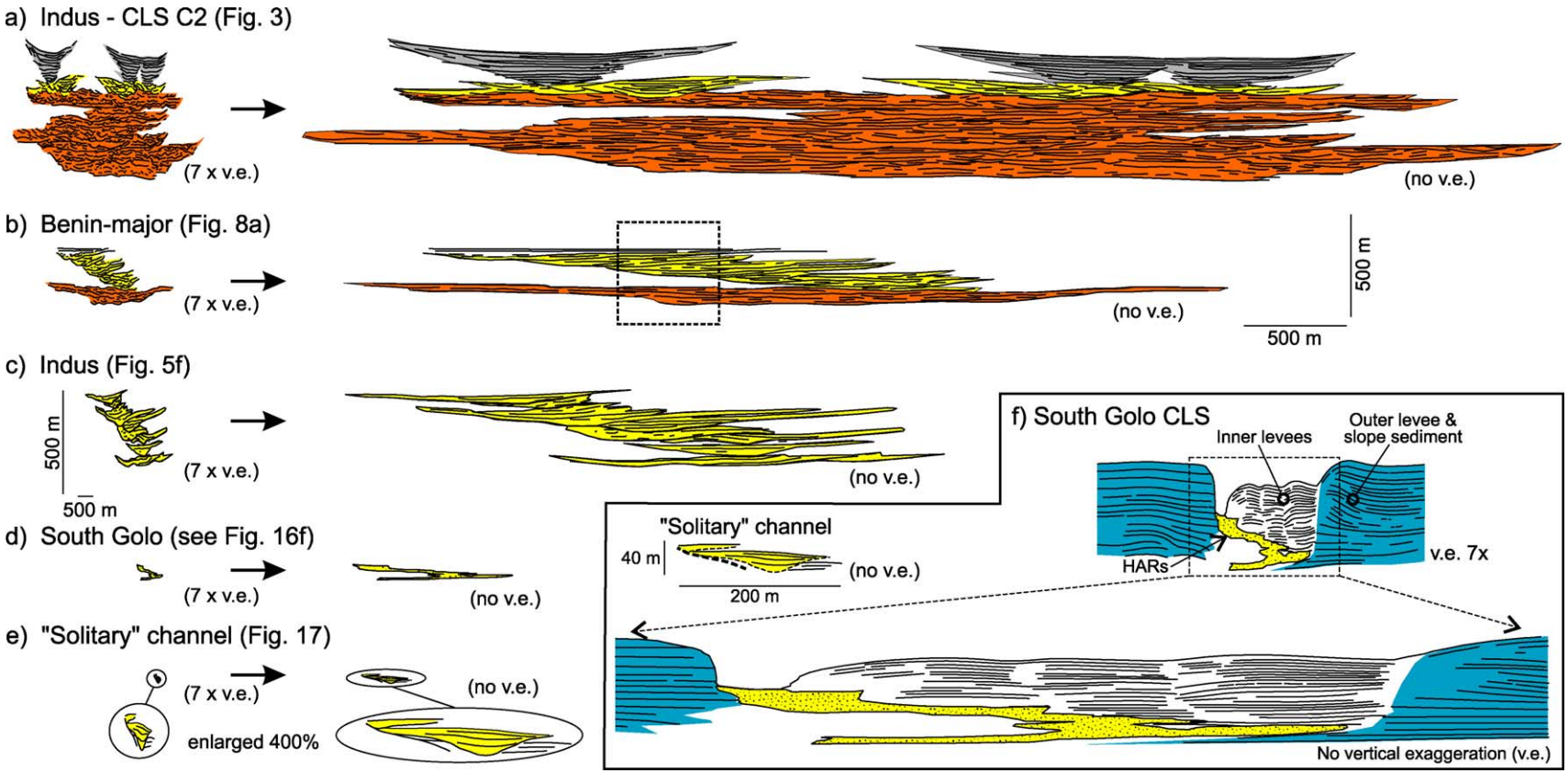

Fig. 16. Line drawing scaled comparisons of HARs from (a) CLS C2 (Indus Fan), (b) Benin-major (Niger Delta slope), (c) a deeper CLS located below CLS C1 (Indus Fan), (d) South Golo CLS (offshore eastern Corsica), and (e) a line drawing of the 'Solitary' channel (SE Spain - drawing based on photo mosaic in Fig. 17). Note that the HARs to the left of the arrows are shown at seven times vertical exaggeration, whereas the HARs to the right are shown with no vertical exaggeration (a more useful scale for making outcrop comparisons). Note also the wide range of dimensions exhibited for channel-deposits in different systems. Some very small systems like South Golo show similarities in architectural style to much larger systems. A line drawing transect through the proximal South Golo CLS (f), shows strong evidence for inner levee development and aggradational channel deposits. Scaled comparisons to the 'Solitary' channel indicate that the two systems are fairly comparable in size and setting (< 900 m deep narrow trough-shaped basin flanked by mountainous terrain). These observations raise questions about whether systems like the 'Solitary' channel contain inner levees and how to recognize them in outcrops. It may be very difficult to distinguish between periods of passive fill and inner levee deposits.

The CLSs imaged on seismic data in this study are typically shown (and interpreted) at a minimum of 7 × vertical exaggeration. Viewing these systems at a 1:1 vertical to horizontal scale reveals how challenging it can be to identify, for example, vertical aggradation of channels on outcrops, particularly in large systems (e.g. Fig. 16). Consider the 500 m × 500 m box drawn above the Benin-major CLS in Fig. 16(b). If this box represented the extent of outcrop exposure, it is unlikely that the entire succession would be interpreted as the same aggradational system, and even less likely that the unit between the lower orange and upper yellow channel deposits would be interpreted as inner levee deposits.

The 'Solitary' channel, located in southeastern Spain (Tabernas-Sorbas Basin), has been studied in detail by several workers (the reader is directed to Kleverlaan (1989), Cronin (1995), Haughton (2000), and Pickering, Hodgson, Platzman, Clark, & Stephens (2001) for detailed descriptions) and is used here in an attempt to link seismic and outcrop-scale observations. The 'Solitary' channel has an erosive base that incises slope mudstones and marlstones (Fig. 17). The incision represents a first-order erosive surface interpreted to have a near-linear planform geometry (Haughton, 2000), and is inferred to be analogous to the erosional fairway at Benin-major. At least three second-order erosive surfaces, each defining a major channel unit ('channel-form'), stack in an offset multi-storey fashion within the first-order incision (see Haughton, 2000, his Fig. 3 inset). These second-order incisions are inferred to be analogous to u- or v-shaped channel-form HARs at Benin-major.

Haughton (2000) suggested that the first-order incision developed during a period of slope bypass, whereas the second-order incisions were caused by episodic flushing of the erosional conduit as it filled. Episodic flushing resulted in abrupt lateral shifts in the second-order channel position (abrupt migrations) followed by a period of fill within each second-order incision, with sandstone bodies displaying onlap, convergence, and lateral accretion. These observations are consistent with the channel-form stacking architecture observed during phases 2 and 3 at Benin-major, where aggradation and migration commonly occured via alternating periods of second-order incision and channel fill. Where the amount of channel fill is greater than the amount of vertical incision, the net effect is channel-form aggradation (with lateral migration accomplished by variable amounts of cut-bank erosion). Lateral accretion stratal architectures tend to develop within the second-order incisions at the 'Solitary' channel, suggesting that gradual channel migrations occur between episodes of abrupt migrations. The same may be true for our seismic examples, but limited resolution in most cases precludes resolving the fill of individual channel-forms.

The dimensions, length-scale, and setting (10 km wide structurally active E-W trending trough-shaped basin—Haughton, 2000) of the 'Solitary' channel are fairly compatible with the small, modern South Golo CLS, offshore East Corsica (Figs. 16(d)–(f)). The off-set stacking of the two second-order incisions (each defining a 'channel-form') creates a cut-bank on the left margin of the 'Solitary' channel (Fig. 17), while the opposite channel margin grades laterally into shale with thin interbeds of siltstone and sandstone. Were these finer-grained interbedded strata deposited as passive fill (i.e. background sedimentation) as suggested by Haughton (2000) and Pickering et al. (2001), or could some of these deposits represent inner levee facies, as observed in the South Golo CLS (Fig. 16(f))? Inner levees also form important elements in several other small, modern active-margin fans, including La Jolla and Hueneme (both off California); it is not unrealistic then to question whether the 'Solitary' channel also contains inner levees. Clearly, the distinction between inner levee and passive fill deposits has important implications for interpreting the evolution of the 'Solitary' channel, and in particular for drawing time-lines through the channel fill. What criteria to use to distinguish between the two, however, is not clear at this point.

4.7. General changes in flow character through time—Benin-major

What causes a system to evolve from a wide erosional fairway bordered by outer levees, to a narrow confined channel bordered by inner levees, ultimately reflects changes in gravity flow character through time. Channel-levee geometry at Benin-major is used here to infer general changes in flow character through its development.

The incision of the erosional fairway suggests that gravity flows were most erosive during its early history. Erosion began initially during the passage of mass transport deposits, eventually leading to vertical incision of the erosional fairway (see also Coleman, Prior, & Lindsay, 1983). Clark and Pickering (1996), Hubscher et al. (1997), Friedmann (2000), Badalini, Kneller, and Winker (2000), Mayall and Stewart (2000), and Kolla et al. (2001) have also reported erosion at the base of other systems. In contrast to other studies, however, sinuous, cross-cutting erosional channels are preserved on the floor of the erosional fairway at Benin-major. This implies that the basal portion of flows traveled down sinuous paths as they erosionally deepened, and largely bypassed, the fairway floor. It also indicates that sinuous channels can also be highly erosive. During the phase 1 fill, the apparent synchronous deposition of the lower outer levees indicates that flows must have been thick enough to overbank the erosional fairway margins. Using the height difference between the lower outer levee crests and the thalweg of the erosional fairway, a lower limit ranging from 200 to 350m would have been required for flows to overbank to outer levee crests during the earliest period of fill. Any sediment accumulation within the erosional fairway would reduce this predicted value.

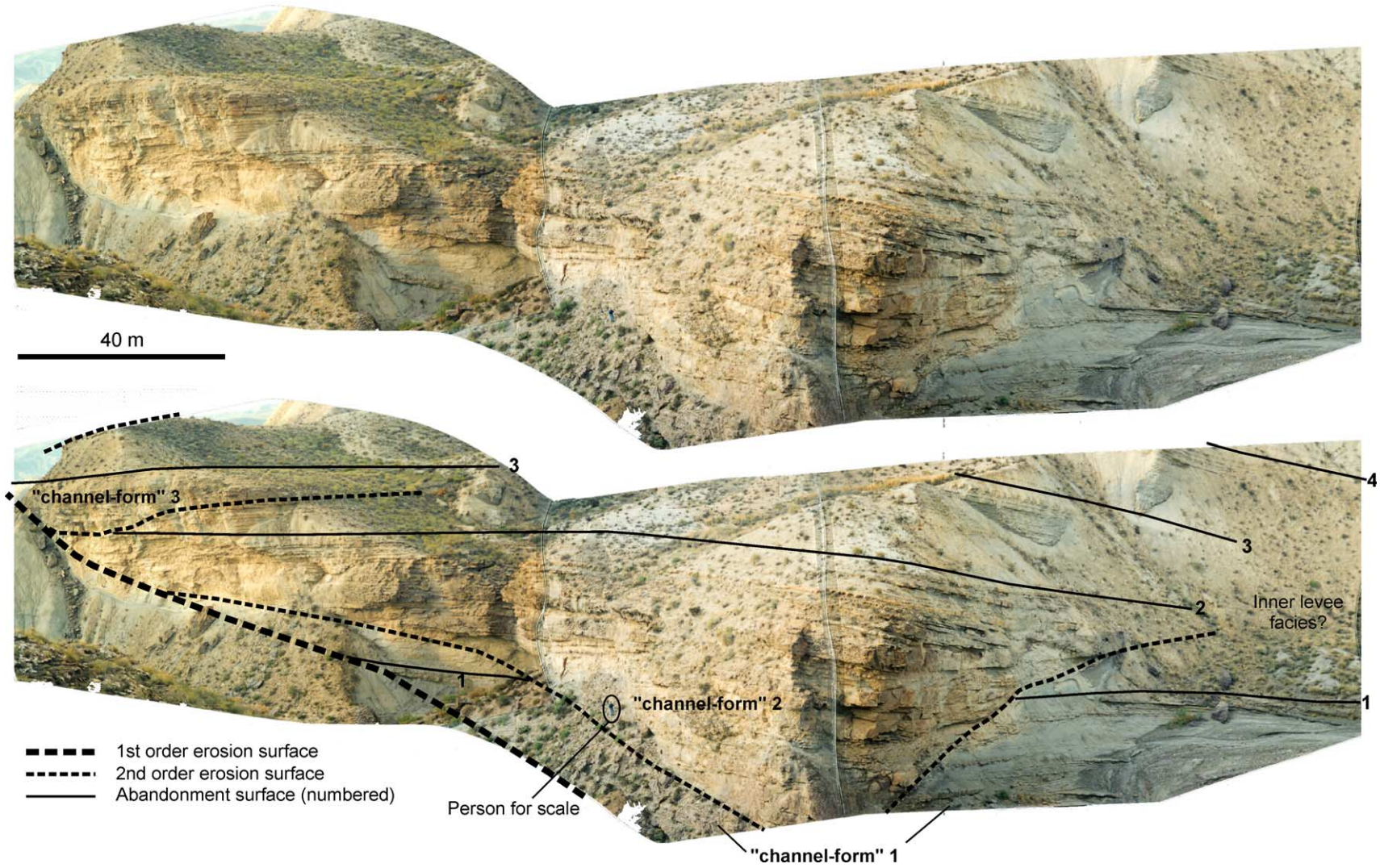

Fig. 17. (a) Uninterpreted and (b) interpreted photo mosaic of the 'Solitary' channel, in SE Spain (Site 2 of Cronin, 1995). A first-order erosive surface is identified along the left-hand margin. Two second-order erosive surfaces are also shown, each defining the base of major channel units inferred to be similar to 'channel-forms' described for Benin-major. Channel-form 2 of the 'Solitary' channel is the only one exposed along both of its margins. It incises channel-form 1 and has a maximum thickness of 25 m and a width of 150 m. Channel-form 2 consists of coarse-grained to conglomeratic deposits, containing mud rip-up clasts and cobbles that are overlain by coarse-grained sandy turbidites and intervals of finer-grained sediment (Cronin, 1995; Haughton, 2000; Pickering et al., 2001). Sandstone bodies within second-order incisions display onlap, convergence, and lateral accretion, and may be separated by third-order erosive surfaces.

In contrast to phase 1, the development of inner levees during phases 2 and 3 caused a reduction in channel cross-sectional area, a proxy for the size of throughput turbidity currents (Pirmez, 1994). The high amplitude seismic reflection that defines the top of the lower outer levee is interpreted as a condensed interval that marks the change from large, erosive flows (phase 1), to smaller, under-fit flows that rarely overbanked the outer levee crests (phase 2). Reflections near the base of many inner levees are inclined towards the channel-axis or are flat lying, and terminate abruptly as onlap onto the erosional fairway or outer levee walls (e.g. Fig. 4(c)). These inner levees are inferred to be from flows that were completely confined between the outer levee crests. In contrast, as the channel floor aggraded (particularly during phase 3), reflections near the tops of some inner levees are inclined away from the channel-axis, sometimes forming wedge-shaped geometries characteristic of less confined flows. Reflections within these inner levees can sometimes be correlated out onto the outer levees (e.g. Figs. 4(c) and 8), indicating that flows once again overbanked the lower outer levee crests. These observations indicate a transition from confined flows during early inner levee deposition, to flows that were not completely contained within the conduit later on, after a period of channel and inner levee aggradation.

Approximations for through-channel flow thickness during fill phases 2 and 3 can be made in areas where inner levee horizons can be correlated into equivalent channel-form horizons (i.e. where there is continuity between inner levee and channel-floor deposits, typically on the inside bend of meanders). The maximum height of inner levee markers above the channel thalweg yields a minimum approximate flow thickness on the order of 120–150 m during phase 2, decreasing to 50–75 m just prior to the abandonment of the system. The estimated decrease in flow thickness between fill phases 1 through 3, combined with the decrease in cross-sectional area, are consistent with McHargue (1991) who predicted a decrease in flow volume during the evolution of CLSs on the Indus Fan.

Although apparently much thinner (80 m thick) than the CLSs described in this paper, the most recently active CLS on the Bengal Fan is characterized by a 14 km wide erosional channel flanked by outer levees, which narrows to a less than 1 km wide channel bordered by inner levees (Hubscher et al., 1997). Using ^{14}C dates from shallow piston cores, Weber, Wiedicke, Kudrass, Hubscher, and Erlenkeuser (1997) interpreted outer levee growth to have ceased at the end of the last glacial maximum, whereas inner levee growth occurred later, during rising sea level in the Holocene. Based on this information, it is reasonable to infer that the erosive base of the system developed during the falling stage of sea level, when sediment supply to the shelf break and slope instability were probably the greatest. The under-fit narrower channels flanked by inner levees, then, would correspond to periods of reduced sediment supply during rising sea level (Hubscher et al., 1997).

Understanding the cause for the apparent decrease in gravity flow size and erosiveness in the Benin-major CLS, however, is hindered because of the lack of core data and age control. There is uncertainty about whether Benin-major evolved through a single cycle or multiple cycles of sea level fluctuation. Its evolution may reflect a combination of changing sea level position and evolving sediment source characteristics (sediment supply, grain size, proximity to the canyon head, etc.), that may or may not be intimately related. These variables, in turn, are believed to have caused changes in gravity flow character through time (including flow composition, size, erosiveness, frequency, and perhaps triggering mechanisms—Piper and Normark, 2001). The precise nature of these changes, and their impact on channel-levee architecture, are still being investigated.

4.8. Architectural variability

Although similar configurations of architectural elements are observed at multiple scales, the detailed geometry of individual elements and their geology can vary from one system to another, or even within different reaches of the same system. Variations include the thickness and inclination of outer levees, the presence or absence of sediment waves, the depth of incision of the erosional fairway, and the planform geometry and grain-size characteristics of channel deposits. Architectural element variability probably reflects some of the controls described by Piper and Normark (2001), including the volume, grain-size, and dominant triggering mechanisms for flows, and the interaction of those flows with pre-existing channel and basin/sea floor morphology (gradients, bathymetric obstacles, etc.).

The geometry of one architectural element may have a strong impact on the geometry of another architectural element or suite of elements. As a result, architectural relationships may be observed between some elements. For example, where the depth of incision of the erosional fairway is large, the thickness of contemporaneous outer levees (at the levee crest) tends to be small, and vice-versa. This apparent inverse relationship probably reflects the ability of through-channel turbidity currents to overbank the margins of the erosional fairway. In some systems, the erosional fairway may be too deeply incised to allow flows to overbank (in which case we would call the incision a canyon). Such systems may only develop outer levees after a period of deposition within the erosional fairway. As a result, the timing for the start of outer levee deposition may vary from one system to another.

A deeply incised erosional fairway may also promote the development of inner levees, by increasing the potential for confinement (and thus under-fitting) of flows. In contrast, systems with a very shallow erosional fairway may develop confined inner levees only during periods of abrupt lateral channel migration or above meander cut-offs. Aggradational HARs in systems that do not have an erosive base may be flanked directly by outer levees (e.g. Fig. 5(f)). Such

systems may be characterized by sheet or channeled-sheet deposits at their base, rather than an erosional fairway (an architecture that is believed to be more common in middle to lower fan settings). The amount of incision at the base of a CLS, early in its history, therefore has a significant impact on its final architecture.

The evolutionary trends shown for the Benin-major CLS, if assumed to be 'normal' (i.e. using it as a baseline for comparison), can be perturbed by events like upper fan avulsions that can terminate the evolution of the system down-dip of the avulsion site (in effect freezing it). Alternatively, a large mass transport complex, deposited within an erosional fairway, could heal over the confinement (i.e. fill the erosional fairway) that may have otherwise lead to the development of inner levees. A similar result could be accomplished by an extended period of muddy slope deposition within the proximal reaches of an erosional fairway.

Complex architectural styles can also be generated if a system enters into an under-fit phase with deposition of inner levees and narrow aggradational channels, and then switches back to a highly erosive phase. Such a scenario may explain the more complicated architecture observed in CLSs C2 and C3 on the Indus Fan (e.g. Fig. 4). The 'normal' evolution of systems can also be perturbed by active structural deformation at the sea floor. Such deformation can trigger rotational slump blocks along the unstable margins of the system, which could plug the channel-axis and perturb the lateral migration of channels. In all cases, different architectural styles from that described for Benin-major would be generated.

Some apparent variations in CLS architecture may also reflect the stage in the 'normal' evolution the system is in. We have demonstrated that the planform and cross-sectional channel geometry at Benin-major evolves through time. The modern slope off West Africa is crossed by several CLSs of various dimensions and in various 'stages' of fill. Some systems are empty erosional conduits (e.g. similar to phase 1 at Benin-major—Fig. 7(a)), others contain deep narrow channels flanked by inner levees (e.g. similar to phase 2 at Benin-major), and still others are nearly entirely filled, with little remaining relief (e.g. similar to the modern sea floor expression of Benin-major—Fig. 7(b)). Comparisons between the final cross-sectional and planform channel geometry at Benin-major (late phase 3—low channel-margin relief, well developed sinuosity), to the present-day modern 'empty' Zaire or Indus fans (with channel floors as much as 400 m below levee crests), for example, may not be meaningful. Instead, a better comparison may be made with phase 2 at Benin-major, when the system had a similar cross-sectional geometry (albeit smaller) as the upper fan CLSs on the modern Zaire and Indus fans.

Finally, the architectural styles described in this paper are from the upper fan reaches of CLSs. Down-fan changes in style are expected (e.g. a decrease in erosional fairway depth and inner levee height; a transition from incision to sheet-like deposition at the base of CLSs, etc.), but have not yet been investigated in detail.

5. Conclusions

(1) Several common architectural elements are recognized in upper fan settings, just outboard the canyon mouth in CLSs C1, C2, and C3 of Indus Fan, and the Benin-major CLS on the western Niger Delta slope. These elements include outer levees, inner levees, erosional fairways, channel-axis deposits, slump blocks, and mass transport deposits.

(2) Vertical, sub-vertical, and lateral stacking patterns of sinuous and/or meandering channel-axis deposits create a range of narrow and wide zones of HARs that vary in acoustic character from discontinuous-chaotic (D-C HARs), to continuous-parallel (C-P HARs), or can appear as isolated channel-forms filled with variable seismic facies. HAR width is controlled by the original width of the channel and the ratio between vertical aggradation and lateral migration of the channel floor. Wide HARs, therefore, either originate from wide channels or from narrow channels that have migrated significantly laterally, with little vertical aggradation. The latter are believed to share the most similarities with fluvial meander-belts, including the development of point bars.

(3) Pulses of rapid channel migration can occur within short channel segments, at any point in the channels aggradational history. They result in local widening of the HARs, the development of prominent cut-banks, and the deposition of a new inner levee opposite the cut-bank. Inner levees are primary architectural elements in many CLSs. Their intimate relationship with channel-axis deposits provides insight into how channels migrate and aggrade through time. Onlapping by inner levees also helps to stabilize the margins of the erosional fairway as it fills.

(4) The early history of the Benin-major CLS is characterized by incision of the erosional fairway. The initial development of outer levees in this system appears to be synchronous with the late incision of the erosional fairway or its early fill history (phase 1). Three phases of channel-deposit evolution are recognized within the erosional fairway. Phase 1 is characterized by a wide unit of D-C HARs that consist of several cross-cutting and amalgamated sinuous channel segments deposited within the erosional fairway. Slumps from the outer levee or erosional fairway walls may be most abundant in this interval. Phase 2 is characterized by narrower D-C and/or stacked channel-form HARs with tortuous sinuosities, bordered by highly aggradational inner levees. Phase 3 is characterized by narrow D-C and/or stacked channel-forms, with well developed meander

loops bordered by inner levees. Phase 3 channel floor deposits aggraded at a faster rate than either the inner or outer levees, resulting in a progressive reduction in channel relief prior to abandonment.

(5) The similarities in first-order architectural elements in upper fan settings in a wide range of CLSs suggest that similar channelized flow processes exist at different scales. Although the evolution presented for the Benin-major CLS is not intended to be a general model, similar architectural element configurations are repeated in several CLSs around the world, suggesting that common evolutionary trends do exist. Many CLSs experience an early incisional history inferred to result from the passage of large, erosive flows. The same systems commonly experience a later period of channel-belt aggradation characterized by narrow channels flanked by confined inner levees, inferred to result from the passage of smaller, under-fit flows. The cause of the switch from dominantly erosive to dominantly depositional is not well understood, but probably reflects a combination of sea level position and an evolving sediment source area. An important control on the final architecture of many CLSs appears to be the amount of incision, if any, that takes place early in its history.

Acknowledgements

We thank Mike Stovall, Peter Swinburn, and Andre Coffa who provided help in the early stages of the project, Patrick McVeigh for logistical assistance, and Brad Prather, Ciaran O'Byrne, Jeremy Willson, Charlie Winker, Craig Shipp, Andrew MacRae, and David Piper for helpful discussions. Tim McHargue, David Jennette and Ven Kolla are thanked for their thoughtful reviews, which improved the manuscript. Shell International E&P, Shell Pakistan, ExxonMobil and the Nigerian National Petroleum Company are thanked for permission to publish these results. Funding for MED was provided by Shell International E&P, a Natural Sciences and Engineering Research Council of Canada (NSERC) post-graduate scholarship, an AAPG grant-in-aid, and a supplemental NSERC scholarship from Natural Resources Canada.

References

Abreu, V., Sullivan, M., Mohrig, D., & Pirmez, C. (2003). Lateral accretion packages (LAPs): an important reservoir element in deep water sinuous channels. *Marine and Petroleum Geology*, this issue (doi: 10.1016/j.marpetgeo.2003.08.003).

Allen, J. R. L. (1964). The Nigerian continental margin: bottom sediments, submarine morphology and geological evolution. *Marine Geology*, *1*, 289–332.

Badalini, G., Kneller, B., & Winker, C. D. (2000). Architecture and processes in the late Pleistocene Brazos-Trinity turbidite system, Gulf of Mexico continental slope. In P. Weimer, R. M. Slatt, J. Coleman, N. C. Rosen, H. Nelson, A. H. Bouma, M. J. Styzen, & D. T. Lawrence (Eds.), (pp. 16–34). *Deep-water reservoirs of the world: GCSSEPM Foundation 20th Annual Research Conference*.

Bellaiche, G., Droz, L., Coutellier, V., Berthon, J.-L., Orsolini, P., Ravenne, C., Aloisi, J.-C., Got, H., & Monaco, A. (1984). Detailed morphology, structure and main growth pattern of the Rhône deep-sea fan. *Marine Geology*, *55*, 181–193.

Bellaiche, G., Droz, L., Gaullier, V., & Pautot, G. (1994). Small submarine fans on the eastern margin of Corsica: Sedimentary significance and tectonic implications. *Marine Geology*, *117*, 177–185.

Bouma, A. H., Coleman, J. M., & DSDP Leg 96 Shipboard Scientists, (1985). Mississippi fan: Leg 96 program and principal results. In A. H. Bouma, W. R. Normark, & N. E. Barnes (Eds.), *Submarine fans and related turbidite systems* (pp. 247–252). New York: Springer-Verlag.

Clark, J. D., & Pickering, K. T. (1996). Submarine channels: processes and architecture. *AAPG Bulletin*, *80*, 194–221.

Clift, P. D., Shimizu, N., Layne, G. D., Blusztajn, J. S., Gaedicke, C., Schlüter, H.-U., Clark, M. K., & Amjad, S. (2001). Development of the Indus Fan and its significance for the erosional history of the Western Himalaya and Karakoram. *Geological Society of American Bulletin*, *114*, 1039–1051.

Coleman, J. M., Prior, D. B., & Lindsay, J. F. (1983). Deltaic influcences on shelfedge instability processes. In D. J. Stanely, & G. T. Moore (Eds.), *The shelfbreak: Critical interface on continental margins* (pp. 121–137). *SEPM Special Publication No. 33*, Tulsa.

Cronin, B. T. (1995). Structurally-controlled deep sea channel courses: examples from the Miocene of southeast Spain and the Alboran Sea, southwest Mediterranean. A. J.Hartley, D. J.Prosser, *Geol. Soc. Special Publication*, *94*, 115–135.

Damuth, J. E., & Flood, R. D. (1985). Amazon Fan, Atlantic Ocean. In A. H. Bouma, W. R. Normark, & N. E. Barnes (Eds.), *Submarine fans and related turbidite systems* (pp. 97–106). New York: Springer-Verlag.

Damuth, J. E., Kowsmann, R. O., Flood, R. D., Belderson, R. H., & Gorini, M. A. (1983). Age relationships of distributary channels on Amazon deep-sea fan: Implications for fan growth pattern. *Geology*, *11*, 470–473.

Deptuck, M. E (2000). The Mara turbidite fan system in the Jeanne d'Arc Basin: Architecture, evolution, and modern analogues. Conference CD with Extended Abstracts, GeoCanada 2000, Calgary, Alberta, May 28–June 2 2000, Abstract number 679

Doust, H., & Omatsola, E. (1989). Niger Delta. J. D. Edwards, P. A. Santogrossi, *AAPG Memoir*, *48*, 201–238.

Droz, L., & Bellaiche, G. (1991). Seismic facies and geologic evolution of the central portion of the Indus Fan. In P. Weimer, & M. Link (Eds.), *Seismic facies and sedimentary processes of submarine fans and turbidite systems* (pp. 383–402). New York: Springer-Verlag.

Droz, L., Rigaut, F., Cochonat, P., & Tofani, R. (1996). Morphology and recent evolution of the Zaire turbidite systems (Gulf of Guinea). *Geological Society of American Bulletin*, *108*, 253–269.

Emmel, F. J., & Curray, J. R. (1985). Bengal Fan, Indian Ocean. In A. H. Bouma, W. R. Normark, & N. E. Barnes (Eds.), *Submarine fans and related turbidite systems* (pp. 107–112). New York: Springer-Verlag.

Flood, R. D. (1987). Side echoes from a sinuous fan channel obscure the structure of submarine fan channel levee systems. *Amazon Fan: Geo-Marine Letters*, *7*, 15–22.

Flood, R. D., Piper, D. J. W., & Shipboard Scientific Party, Klaus, A., (1995). Site 934. In R. D. Flood, D. J. W. Piper, & A. Klaus (Eds.), (*155*) (pp. 241–271). *Proceedings of the Ocean Drilling Program, Initial Reports*.

Friedmann, S. J (2000). Recent advances in deep-water sedimentology and stratigraphy using conventional and high-resolution 3D seismic data. Conference CD with Extended Abstracts, GeoCanada 2000, Calgary, Alberta, May 28–June 2, 2000

Garner, J. V., Bohannon, R. G., Field, M. E., & Masson, D. G. (1996). The morphology, processes, and evolution of Monterey Fan: A revisit. In J. V. Gardner, M. E. Field, & D. C. Twitchell (Eds.), *Geology of*

the United States Seafloor: The view from GLORIA (pp. 193–220). New York: Cambridge University Press.

Hackbarth, C. J., & Shew, R. D. (1994). *Morphology and stratigraphy of a mid-Pleistocene turbidite leveed channel from seismic, core and log data. Submarine Fans and Turbidite Systems: GCSSEPM Foundation 15th Annual research Conference, Northeastern Gulf of Mexico*, p. 127–133.

Haughton, P. D. W. (2000). Evolving turbidite systems on a deforming basin floor, Taberna, SE Spain. *Sedimentology*, *47*, 497–518.

Hiscott, R. N., Hall, R. R., & Pirmez, C. (1997). Turbidity-current overspill from the Amazon Channel: texture of the silt/sand load, paleoflow from anisotropy of magnetic susceptibility, and implications for flow processes. In R. D. Flood, D. J. W. Piper, A. Klaus, & L. C. Peterson (Eds.), (*Vol. 155*) (pp. 53–78). *1997 Proceedings of the Ocean Drilling Program, Scientific Results*.

Hubscher, C., Spieb, V., Breitzke, M., & Weber, M. E. (1997). The youngest channel-levee system of the Bengal Fan: results from digital sediment echosounder data. *Marine Geology*, *141*, 125–145.

Kastens, K. A., & Shor, A. N. (1985). Depositional processes of a meandering channel on Mississippi fan. *AAPG Bulletin*, *69*, 190–202.

Kenyon, N. H., Amir, A., & Cramp, A. (1995). Geometry of the younger sediment bodies of the Indus Fan. In K. T. Pickering, R. N. Hiscott, N. H. Kenyon, F. Ricci Lucchi, & R. D. A. Smith (Eds.), (pp. 89–93). *Atlas of deep water environments: Architectural style in turbidite systems*, London: Chapman and Hall.

Kleverlaan, K. (1989). Three distinctive feeder-lobe systems within one time slice of the Tortonian Tabernas fan, SE Spain. *Sedimentology*, *36*, 25–45.

Kolla, V., & Coumes, F. (1987). Morphology, internal structure, seismic stratigraphy, and sedimentation of Indus Fan. *AAPG Bulletin*, *71*, 650–677.

Kolla, V., Bourges, Ph., Urruty, J.-M., & Safa, P. (2001). Evolution of deep-water Tertiary sinuous channels offshore Angola (west Africa) and implications for reservoir architecture. *AAPG Bulletin*, *85*, 1373–1405.

Manley, P. L., Pirmez, C., Busch, W., & Cramp, A. (1997). Grain-size characterization of Amazon Fan deposits and comparison to seismic facies units. In R. D. Flood, D. J. W. Piper, A. Klaus, & L. C. Peterson (Eds.), (*155*) (pp. 35–52). *1997 Proceedings of the Ocean Drilling Program, Scientific Results*.

Mayall, M., & Stewart, I. (2000). The architecture of turbidite slope channels. In P. Weimer, R. M. Slatt, J. Coleman, N. C. Rosen, H. Nelson, A. H. Bouma, M. J. Styzen, & D. T. Lawrence (Eds.), (pp. 578–586). *Deep-water reservoirs of the world: GCSSEPM Foundation 20th Annual Research Conference*.

McHargue, T. R. (1991). Seismic facies, processes, and evolution of Miocene inner fan channels, Indus Submarine Fan. In P. Weimer, & M. Link (Eds.), *Seismic facies and sedimentary processes of submarine sans and turbidite systems* (pp. 402–413). New York: Springer-Verlag.

McHargue, T. R., & Webb, J. E. (1986). Internal geometry, seismic facies, and petroleum potential of canyons and inner fan channels of the Indus Submarine Fan. *AAPG Bulletin*, *70*, 161–180.

Mutti, E., & Normark, W. R. (1991). An integrated approach to the study of turbidite systems. In P. Weimer, & M. H. Link (Eds.), *Seismic facies and sedimentary processes of modern and ancient submarine fans* (pp. 75–106). New York: Springer-Verlag.

Naini, B. R., & Kolla, V. (1982). Acoustic character and thickness of sediments of the Indus Fan and the continental margin of western India. *Marine Geology*, *47*, 181–195.

Nakajima, T., Satoh, M., & Okamura, Y. (1998). Channel-levee complexes, terminal deep-sea fan and sediment wave fields associated with the Toyama deep-sea channel system in the Japan Sea. *Marine Geology*, *147*, 25–41.

Nissen, S. E., Haskell, N. L., Steiner, C. T., & Coterill, K. L. (1999). Debris flow outrunner blocks, glide tracks, and pressure ridges identified on the Nigerian continental slope using 3-D seismic coherency. *The Leading Edge, May 1999*, 595–599.

Normark, W. R. (1970). Growth patterns of deep sea fans. *AAPG Bulletin*, *54*, 2170–2195.

Normark, N. R. (1978). Fan valleys, channels, and depositional lobes on modern submarine fans: characters for recognition of sandy turbidite environments. *AAPG Bulletin*, *62*, 912–931.

Normark, W. R., Piper, D. J. W., Posamentier, H., Pirmez, C., & Migeon, S (2003). Variability in form and growth of sediment waves on turbidite channel levees, *Marine Geology*, 192, 23–58.

O'Connell, S., McHugh, C., & Ryan, W. B. F. (1995). Unique fan morphology in an entrenched thalweg channel on the Rhone Fan. In K. T. Pickering, R. N. Hiscott, N. H. Kenyon, F. Ricci Lucchi, & R. D. A. Smith (Eds.), *Atlas of deep water environments: Architectural style in turbidite systems* (pp. 80–83). Chapman and Hall: London.

Pichevin, L (2000). Etude sédimentaire et sismique d'un éventail turbiditique sableux: le systèm récent du Golo (Marge Est-Corse). DEA Environnements et Paléoenvironnements Cotiers et Océaniques, Université Bordeaux, 57 p

Pickering, K. T., Hodgson, D. M., Platzman, E., Clark, J. D., & Stephens, C. (2001). A new type of bedform produced by backfilling processes in a submarine channel, Late Miocene, Tabernas-Sorbas Basin, SE Spain. *Journal of Sediment Research*, *71*, 692–704.

Piper, D. J. W., Hiscott, R. N., & Normark, W. R. (1999). Outcrop-scale acoustic facies analysis and the latest Quaternary development of Hueneme and Dume submarine fans, offshore California. *Sedimentology*, *46*, 47–78.

Piper, D. J. W., & Deptuck, M. E. (1997). Fine-grained turbidites of the Amazon Fan: facies characterization and interpretation. In R. D. Flood, D. J. W. Piper, A. Klaus, & L. C. Peterson (Eds.), *1997 Proceedings of the Ocean Drilling Program, Scientific Results* (pp. 79–108).

Piper, D. J. W., & Normark, W. R. (1983). Turbidite depositional patterns and flow characteristics, Navy Submarine fan, California Continental Borderlands. *Sedimentology*, *30*, 681–694.

Piper, D. J. W., & Normark, W. R. (2001). Sandy fans - from Amazon to Hueneme and beyond. *AAPG Bulletin*, *85*, 1407–1438.

Pirmez, C (1994). Growth of a submarine meandering channel-levee system on the Amazon Fan Unpublished Ph.D. Thesis, Columbia University, New York, 587 p

Pirmez, C., Beaubouef, R. T., Friedmann, S. J., & Mohrig, D. C. (2000). Equilibrium profiles and baselevel in submarine channel: Examples from Late Pleistocene systems and implications for the architecture of deepwater reservoirs. In P. Weimer, R. M. Slatt, J. Coleman, N. C. Rosen, H. Nelson, A. H. Bouma, M. J. Styzen, & D. T. Lawrence (Eds.), *Deep-water reservoirs of the world: GCSSEPM Foundation 20th Annual Research Conference* (pp. 782–805).

Posamentier, H.W (2003). Depositional elements associated with a basin floor channel-levee complex: case study from the Gulf of Mexico. *Marine and Petroleum Geology*, this issue

Posamentier, H. W., Meizarwin, Wisman, P. S., & Plawman, T. (2000). Deep water depositional systems—Ultra-deep Makassar Strait, Indonesia. In P. Weimer, R. M. Slatt, J. Coleman, N. C. Rosen, H. Nelson, A. H. Bouma, M. J. Styzen, & D. T. Lawrence (Eds.), (pp. 806–816). *Deep-water reservoirs of the world: GCSSEPM Foundation 20th Annual Research Conference*.

Shepard, F. P., & Emery, K. O. (1973). Congo submarine canyon and fan valley. *AAPG Bulletin*, *57*, 1679–1691.

Skene, K. I (1998). Architecture of submarine channel levees. Unpublished PhD Thesis, Dalhousie University, Halifax, Nova Scotia, 362 pp.

Torres, J., Droz, L., Savoye, B., Terentieva, E., Cochonat, P., Kenyon, N. H., & Canals, M. (1997). Deep-sea avulsion and morphosedimentary evolution of the Rhône Fan Valley and Neofan during the Late Quaternary (north-western Mediterranean Sea). *Sedimentology*, *44*, 457–477.

Vittori, J., Morash, A., Savoye, B., Marsset, T., Lopez, M., Droz, L., & Cremer, M. (2000). The Quaternary Congo deep-sea fan: preliminary results on reservoir complexity in turbiditic systems using 2D high resolution seismic and multibeam data. In P. Weimer, R. M. Slatt, J.

Coleman, N. C. Rosen, H. Nelson, A. H. Bouma, M. J. Styzen, & D. T. Lawrence (Eds.), *Deep-water reservoirs of the world: GCSSEPM Foundation 20th Annual Research Conference* (pp. 1045–1058).

Von Rad, U., & Tahir, M. (1997). Late Quaternary sedimentation on the outer Indus shelf and slope (Pakistan): evidence from high-resolution seismic data and coring. *Marine Geology*, *138*, 193–236.

Walker, R. G. (1978). Deep-water sandstone facies and ancient submarine fans: models for exploration for stratigraphic traps. *AAPG Bulletin*, *62*, 932–966.

Weber, M. E., Wiedicke, M. H., Kudrass, H. R., Hubscher, C., & Erlenkeuser, H. (1997). Active growth of the Bengal Fan during sea-level rise and highstand. *Geology*, *25*, 315–318.